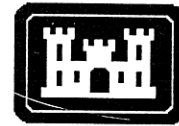




Tests in Ice on an Antarctic Research Vessel Model

Jean-Claude Tatinclaux

February 1992



**U.S. Army Corps
of Engineers**
Cold Regions Research &
Engineering Laboratory

Tests in Ice on an Antarctic Research Vessel Model

Jean-Claude Tatinclaux

February 1992

PREFACE

This report was prepared by Dr. Jean-Claude Tatinclaux, Chief, Ice Engineering Research Branch, Experimental Engineering Division, U.S. Army Cold Regions Research and Engineering Laboratory. The ship model tests in ice reported here were conducted under a Cooperative Research and Development Agreement (CRDA) between North American Shipbuilding, Inc., Larose, Louisiana, and CRREL. The report was technically reviewed by Dr. Devinder S. Sodhi and Dr. James Lever of CRREL.

Alan Reynolds and Kenneth Rea from Offshore Research Ltd., Vancouver, B.C., Canada, are owed many thanks for their help in preparing and instrumenting the ship model and for their suggestions and discussions during the course of the tests. Their total collaboration ensured the full success of the model test program. The author also expresses his gratitude to his many colleagues of the Ice Engineering Research Branch, and to the support services of CRREL, who so willingly lent a hand, often on short notice.

The contents of this report are not to be used for advertising or promotional purposes. Citation of brand names does not constitute an official endorsement or approval of the use of such commercial products.

CONTENTS

	Page
Preface	ii
Nomenclature	v
Introduction	1
CRREL ice test basin	1
Model ice property measurements	3
Flexural strength.....	3
Bulk elastic modulus	4
Crushing strength	5
Ice density	5
Examples of ice property measurements.....	5
Measured properties of test ice sheets	5
Experimental set-up	7
Ship model	7
Measurement transducers	9
Data acquisition system	9
Video and photographic coverage	9
Ice friction tests	10
Resistance tests in level ice	11
General	11
Test procedure	11
Observation and data presentation	12
Data analysis	14
Full-scale resistance predictions	14
Resistance tests in open water.....	16
Overload propulsion tests in open water	17
General	17
Data presentation and analysis	17
Propeller coefficients	18
Propulsion tests in ice	19
Test conditions and procedures	19
Data presentation and analysis	21
Full-scale predictions	25
Direct extrapolation	25
Use of open-water propeller coefficients	26
Use of SSPA test data	26
Backing tests	26
Ridge breaking tests	27
Ridge building procedures	27
Test procedure	29
Ramming tests in thick, level ice	29
Conclusions	31
Literature cited	36
Appendix A: Open-water characteristics of propeller-duct combination	39
Appendix B: Effect of test length on measured ice resistance	41
Abstract	43

ILLUSTRATIONS

Figure	Page
1. Views of CRREL ice tank	2
2. Ice flexural strength measurements	3
3. Modulus of elasticity measurements	4
4. View of indenter to measure ice crushing strength	4
5. Examples of ice property measurements	5
6. Model of Antarctic research vessel	6
7. Ballasted model in trim tank	8
8. Data acquisition system	9
9. Underwater video system	10
10. Friction table	11
11. Results of friction tests	11
12. Sawing the channel	12
13. Sawn channel and general layout	13
14. Breaking pattern at model bow	13
15. Channel behind ship model during resistance tests	14
16. Records of resistance tests	15
17. Nondimensional submergence resistance vs Froude number	15
18. Nondimensional breaking resistance vs two parameters	16
19. Predicted full-scale ice resistance of naked hull	16
20. Results of resistance tests in open water	17
21. Results of bollard tests	18
22. Results of overload tests in open water	19
23. Underwater views during model propulsion tests	20
24. Time history of recorded signals during propulsion tests	22
25. Results of model propulsion tests	25
26. Propulsion characteristics	26
27. Backing tests	27
28. Ridge construction	28
29. Ridge profile	30
30. Model in ridge after first ram	31
31. Imprint of model in ridge after first ram	31
32. Model breaks through ridge at second ram	32
33. Underwater view of model in ridge	32
34. Ramming tests in 100-mm-thick ice	33
35. Underwater views during a ramming test	35
36. Results of model ramming tests	37

TABLES

Table	Page
1. Main characteristics of the Antarctic research vessel	1
2. Measured ice sheet properties	6
3. Results of ice friction tests	11
4. Results of resistance tests in level ice	14
5. Predicted full-scale resistance of naked hull	16
6. Results of open-water resistance tests	17
7. Results of bollard tests	18
8. Results of overload tests	19
9. Results of regression analysis of overload test data	19
10. Results of propulsion tests in level ice	25
11. Results of ramming tests in thick level ice	30

NOMENCLATURE

b	width of flat indenter used to measure ice crushing strength	n	propeller rotational speed
B	width of ice cantilever beams	n_{FS}	propeller speed at full scale
BWL	ship beam at water level	n_{sp}	model propeller speed at self-propulsion point
C_F	frictional resistance coefficient in open water	P	failure load of ice cantilever beam
C_n	ice strength coefficient = $\sigma_f/\gamma h_i$	P_d	delivered power
D	propeller diameter	P_{FS}	delivered power at full scale
D_p	penetration distance in ice during ramming tests	P_{sp}	delivered power at model self-propulsion point
E	ice bulk modulus of elasticity	Q_p	propeller torque
f_i	ice-hull dynamic friction factor	Q_{FS}	propeller torque at full scale
F_c	average crushing force on indenter	Q_{sp}	model propeller torque at self-propulsion point
F_n	Froude number = $V/\sqrt{gh_i}$	R_{app}	appendage resistance in open water
F_N	normal load on ice sample during friction tests	R_{bk}	breaking component of ice resistance = $R_{it} - R_{ps}$
F_T	tangential load on ice sample during friction tests	R_f	ship frictional resistance in water
g	acceleration of gravity	R_i	net resistance in level ice = $R_{it} - R_f = R_s + R_{bk}$
GM	transverse metacentric height	R_{it}	total resistance in level ice
h_i	ice thickness	R_{ow}	total resistance in open water
J	propeller advance coefficient = V/nD	R_{ps}	total resistance in sawn ice
k	coefficient	R_s	submergence component of ice resistance = $R_{ps} - R_f$
KG	distance from center of gravity to keel	S	ship hull wetted area
K_q	propeller torque coefficient	t	thrust deduction factor
K_{td}	duct thrust coefficient	T_p	propeller thrust
K_{tp}	propeller thrust coefficient	T_{sp}	model propeller thrust at self-propulsion point
K_{tt}	thrust coefficient of propeller-nozzle combination	T_t	thrust of propeller-nozzle combination
ℓ_c	ice characteristic length	V	ship speed
L	length of ice cantilever beam	γ	specific weight of water = ρg
LCG	location of center of gravity	η_o	open water propeller efficiency
LOA	overall ship length	λ	model scale
LWL	ship length at waterline	ν	ice Poisson's ratio = 0.3
		ρ	water density
		σ_c	ice crushing strength
		σ_f	ice flexural strength

Tests in Ice on an Antarctic Research Vessel Model

JEAN-CLAUDE TATINCLAUX

INTRODUCTION

The National Science Foundation, charterer of the Antarctic research vessel being built by North American Shipbuilding, Inc. (NASI), of Larose, Louisiana, required model tests in ice to be conducted. These tests were to verify that the vessel would be capable of transiting at 3 kn (1.5 m/s) through 3 ft (0.9 m) of level ice with the installed power. The ice tests were also intended to evaluate the vessel's capability of ramming through pressure ridges and thick ice floes.

The full-scale conditions to be modeled in the ice tests were the following:

1. Towed ice resistance at 2, 3 and 4 kn (1.1, 1.5 and 2.1 m/s) in 3-ft level ice, and at 2, 4 and 6 kn (1.0, 1.5 and 2.1 m/s) in 1.5-ft (0.5-m) level ice.
2. Propulsion tests at 3 kn in 3-ft level ice.
3. Ramming of a pressure ridge having a 6-ft (1.8-m) sail and 20-ft (6.1-m) keel at an impact speed of 8 kn (4.1 m/s).
4. Ramming of 6-ft thick level ice at an impact speed of 6 kn.

In all the above conditions the ice flexural strength was assumed to be 100 lb/in.² (700 kPa).

A model of the Antarctic research vessel was built by Offshore Research Ltd. (ORL), Vancouver, B.C., at a scale of $\lambda = 1:18.18$. This particular scale was selected so that existing fixed-pitch stock propellers could be used to model the 4-m prototype CP propellers. The main full-scale and model characteristics of the vessel are given in Table 1.

Because gravity and inertia are considered the dominant forces in ship-ice interaction, the Froude law of similitude is the scaling law in ice model tests (Tatinclaux 1988). Therefore, all linear dimensions, in particular ice thickness, are scaled by λ . Similarly, all ice mechanical properties such as flexural strength, crushing strength, elastic modulus ought to be scaled by λ . Ship speed is scaled down by $\sqrt{\lambda}$, while model propeller speed is $\sqrt{\lambda}$ times the full-scale values. Correspondingly, all forces are usually scaled by λ^3 , torques by λ^4 and power by $\lambda^{3.5}$.

Table 1. Main characteristics of the Antarctic research vessel.

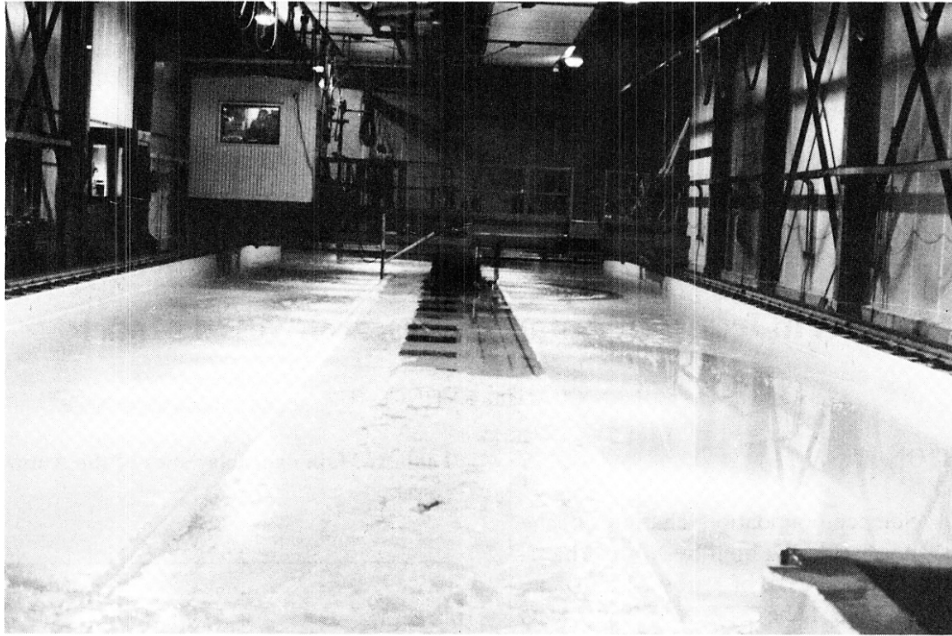
	Full scale	Model (scale 1:18.18)
LOA	93.72 m	5.15 m
LWL	84.73 m	4.66 m
BWL	18.30 m	1.01 m
Draft	6.63 m	0.36 m
Wetted area	2158 m ²	6.53 m ²
LCG	43.89 m	
	fwd from 0 station	2.41 m
KG	7.34 m	0.40 m
GM	1.37 m	0.075 m
Displacement	6417 long tons	1085 kg
Propellers		
	Diameter: 4.0 m	0.22 m
	(Inward, handed in NSMB type 37 nozzles)	
Power	8.8 MW	343.5 W
Rudders		
	Modified high lift "schilling" types	

This report describes briefly CRREL's ice towing tank where the model tests were conducted, the data acquisition system, and model and test set-up. It presents the results of all model tests performed, with extrapolation to full scale when warranted.

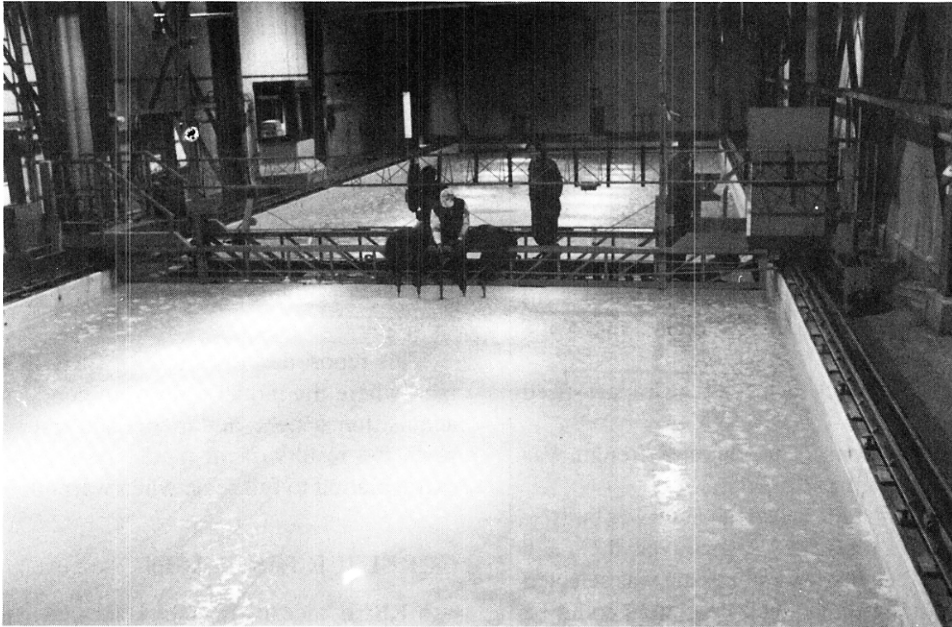
CRREL ICE TEST BASIN

CRREL's ice towing tank is located in the Ice Engineering Facility (IEF). The tank is 120 ft long \times 30 ft wide \times 8 ft deep (36 \times 9 \times 2.4 m). The trim tank is 18 ft long \times 10 ft wide \times 8 ft deep (5.5 \times 3.0 \times 2.4 m). The trim area can be isolated from the main tank by a sliding insulated door. A melt tank (10 \times 30 \times 12 ft [3 \times 9 \times 3.6 m]) is located at the other end of the tank. After tests are completed, the remaining ice is pushed into the melt tank while another ice sheet is grown in the towing tank. Seven forced-air cooling coils can bring the air temperature in the room to a minimum of -10°F (23°C). The refrigeration fluid is ammonia.

A track-and-pinion-driven towing carriage spans the tank. It has a maximum speed of 7 ft/s (2.1 m/s) at a load of 1000 lb (4500 N). A small cabin on the carriage



a. Main towing carriage.



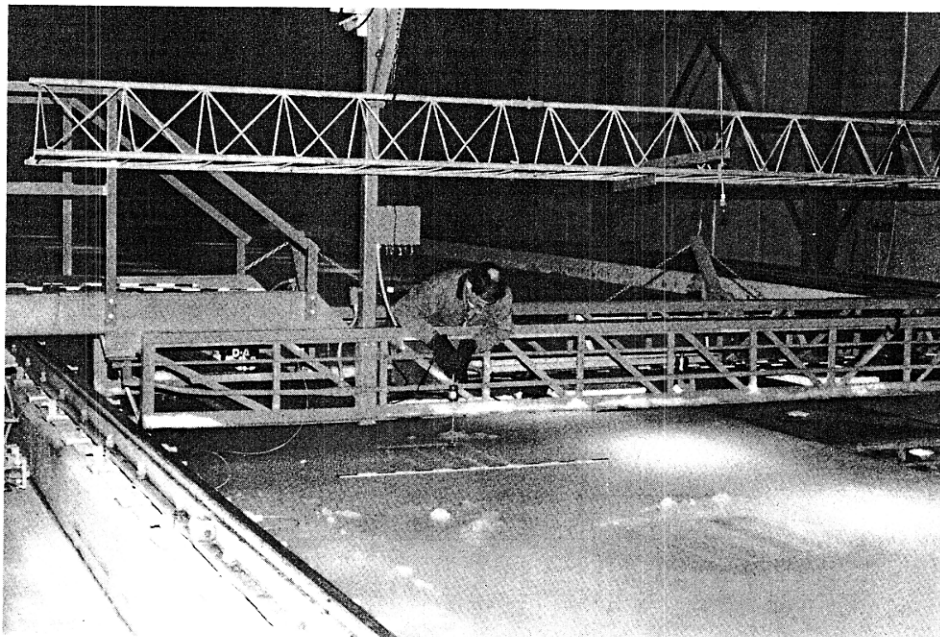
b. Auxiliary carriage.

Figure 1. Views of CRREL ice tank.

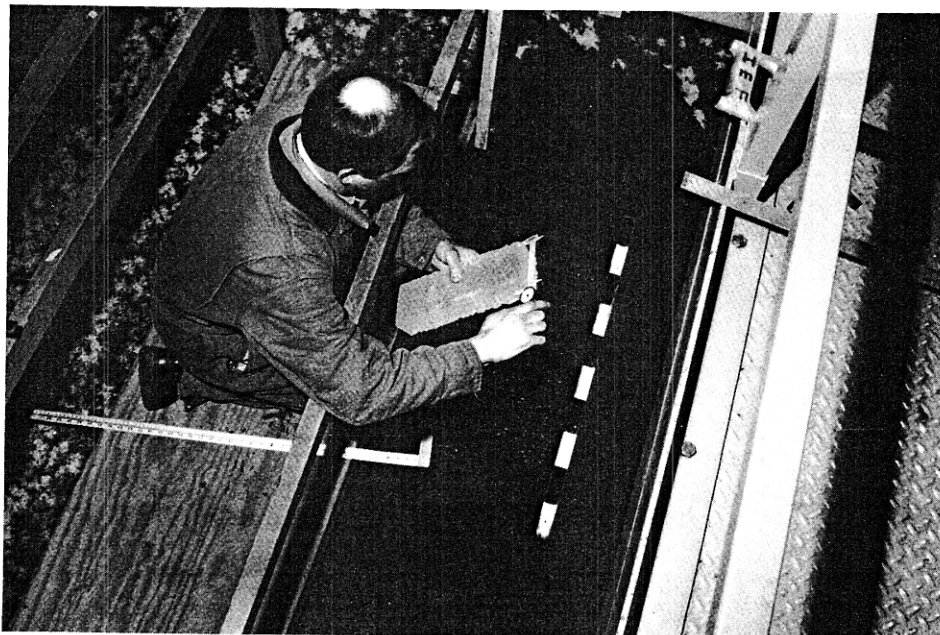
houses the carriage controls and the data acquisition system. The carriage is equipped with seven ice pushers to clear the remaining ice from the tank surface into the melt tank at the end of any series of tests (Fig. 1a). An autonomous personnel carriage is used to carry out ice property measurements prior to tests, and to do a final ice clean up before an ice sheet is seeded (Fig. 1b).

The model ice is grown from a 0.95% urea solution in water. The water is cooled to about -0.1°C , and the water bath is continuously mixed by a system of bubbler

hoses to ensure uniform temperature throughout the water column. The ice sheet is initiated by the wet seeding method at an air temperature of approximately 10°F (-12°C). A thin mist of water is sprayed into the cold air, where it forms an ice fog that settles on the surface of the water to initiate the ice sheet. This method ensures a model ice with a crystallographic structure similar to that of sea ice. The ice sheet is grown at an air temperature between 0 and -10°F (-18 to 23°C) until its thickness is close to the target thickness. The air temper-



a. Applying a downward load.



b. Measuring the broken beam.

Figure 2. Ice flexural strength measurements.

ature in the tank room is then allowed to rise to about 34°F (1°C), and the ice sheet allowed to temper until its flexural strength has reached the target value.

MODEL ICE PROPERTY MEASUREMENTS

Flexural strength

The flexural strength of model ice is measured by the standard method of in-situ cantilever beam tests recommended by ice committees of both IAHR and ITTC

(Schwarz 1979, ITTC 1990). Cantilever beams with length $L = 5$ to $7h_i$ and width $B = 1-2h_i$, where h_i = ice thickness, are sawn in the ice sheet. A downward load is manually applied to the tip of each beam (Fig. 2a) and the failure load P recorded. The dimensions L , B and h_i of the broken beams are measured (Fig. 2b), and the flexural strength calculated as

$$\sigma_f = \frac{6PL}{Bh_i^2} \quad (1)$$

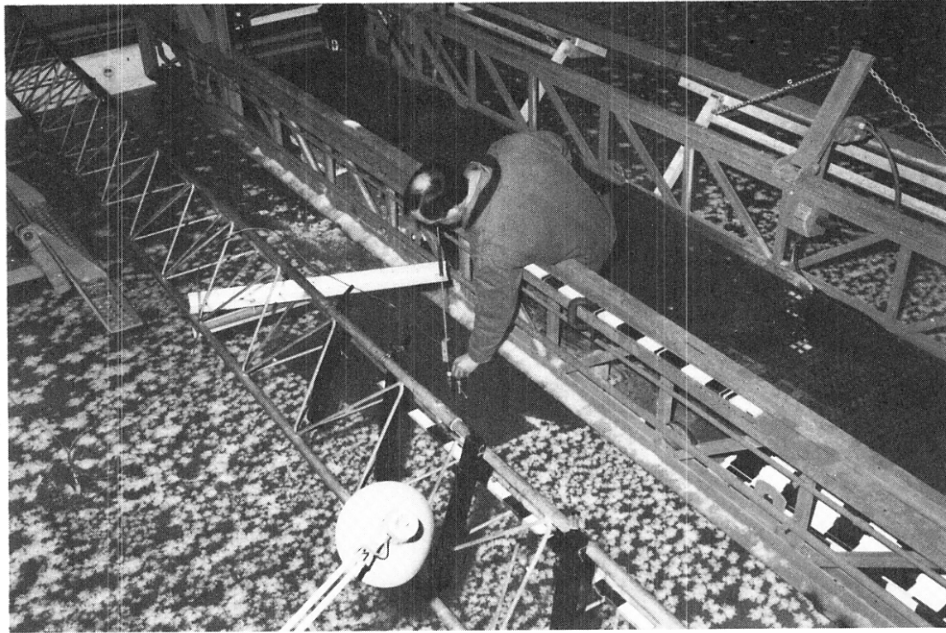


Figure 3. Modulus of elasticity measurements.

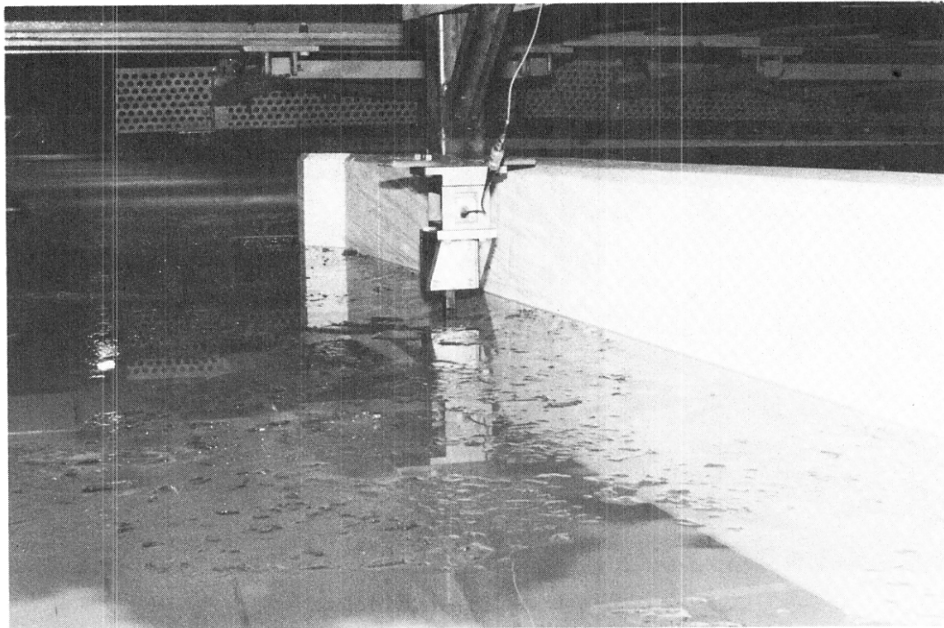


Figure 4. View of indenter to measure ice crushing strength.

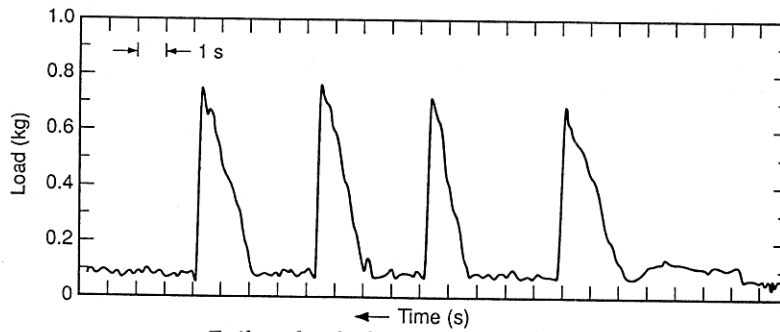
L and B are measured to the nearest millimeter and h_i is measured by a caliper to the nearest half-millimeter. Three to five beams are tested at any one time and the results averaged. The standard deviation on σ_f is usually of the order of 10% of the mean

Bulk elastic modulus

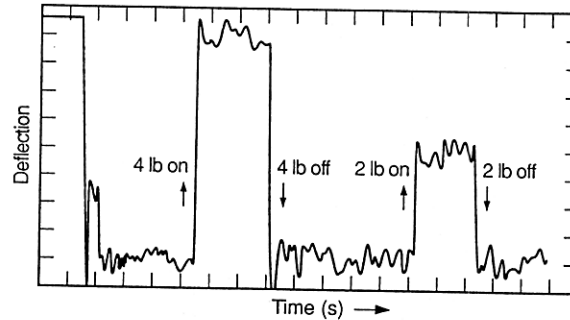
The ice characteristic length ℓ_c and corresponding bulk elastic modulus E are measured in situ by the plate

deflection method (Sodhi et al. 1982). A weight P is applied on the ice sheet and the corresponding deflection of the ice sheet next to the load is measured by a precision LVDT (Fig. 3). The characteristic length ℓ_c is calculated from elastic plate theory and the elastic modulus given by

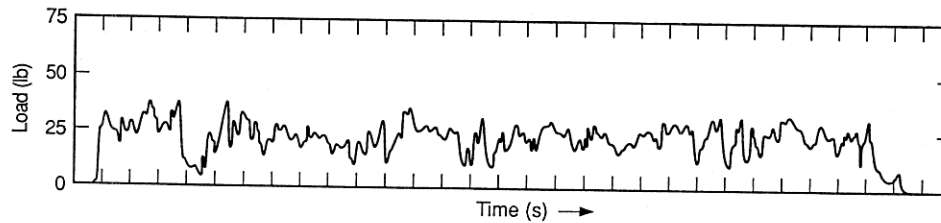
$$E = 12\gamma(1 - \nu^2) \frac{\ell_c^4}{h_i^3} \quad (2)$$



a. Failure load of cantilever beam (σ_f).



b. Deflection of ice sheet (E).



c. Measured force on indenter.

Figure 5. Examples of ice property measurements (test series 500).

where γ = specific weight of water and ν = ice Poisson's ratio = 0.3.

The characteristic length is usually measured with a 10% accuracy, and therefore the modulus has no better than a 40% accuracy. It has been CRREL's experience that the characteristic length of urea model ice is on the order of 10 to 12 ice thicknesses.

Crushing strength

The model ice crushing strength was measured continuously during the tests. A flat indenter ($b = 3/4$ in. [1.9 mm] thick) was towed to the side and rear of the model (Fig. 4). The force exerted by the ice on the indenter was measured by a 50-lb capacity force-block, connected to a chart recorder. The trace on the graph recorder was averaged visually to obtain the average crushing force F_c ; the crushing strength was calculated by

$$\sigma_c = \frac{F_c}{bh_i}$$

Ice density

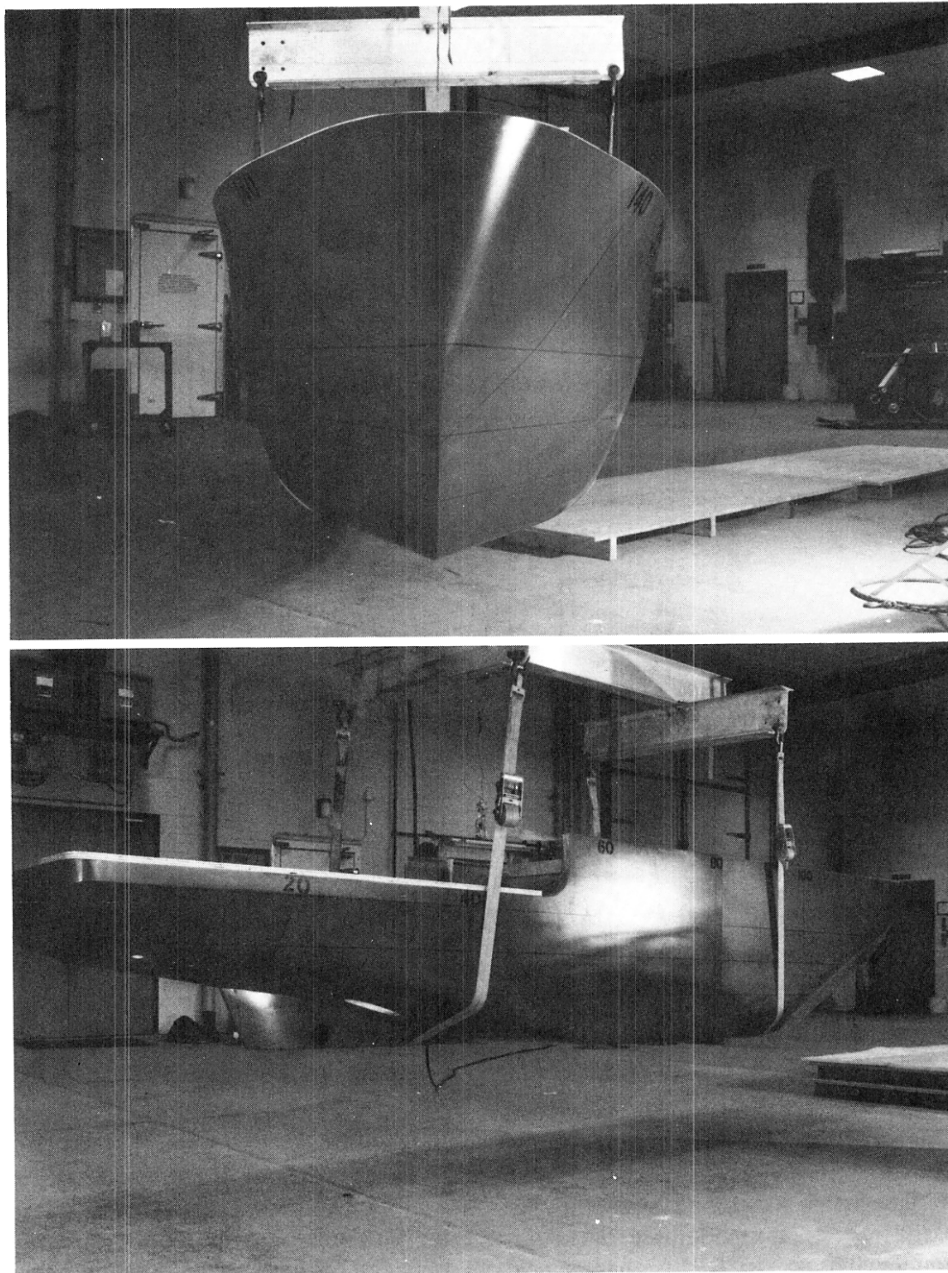
In the present series of model tests, the ice density was not measured. However, past measurements with the same urea model ice have consistently given a value of 0.93 for the ice specific gravity. As in all ice towing tanks, the model ice is relatively denser (or less buoyant) than sea ice, which has a density relative to sea water of 0.89 or less.

Examples of ice property measurements

Figure 5 shows examples of measurements of ice flexural strength, elastic modulus and crushing strength. These particular examples were obtained prior to or during the captive model propulsion tests (test series 500), discussed later.

Measured properties of test ice sheets

In all, four ice sheets were grown—two for resistance tests, one for propulsion tests and the fourth one for ramming tests. The flexural strength was measured for all four sheets, and the elastic modulus and crushing



a. Naked hull.

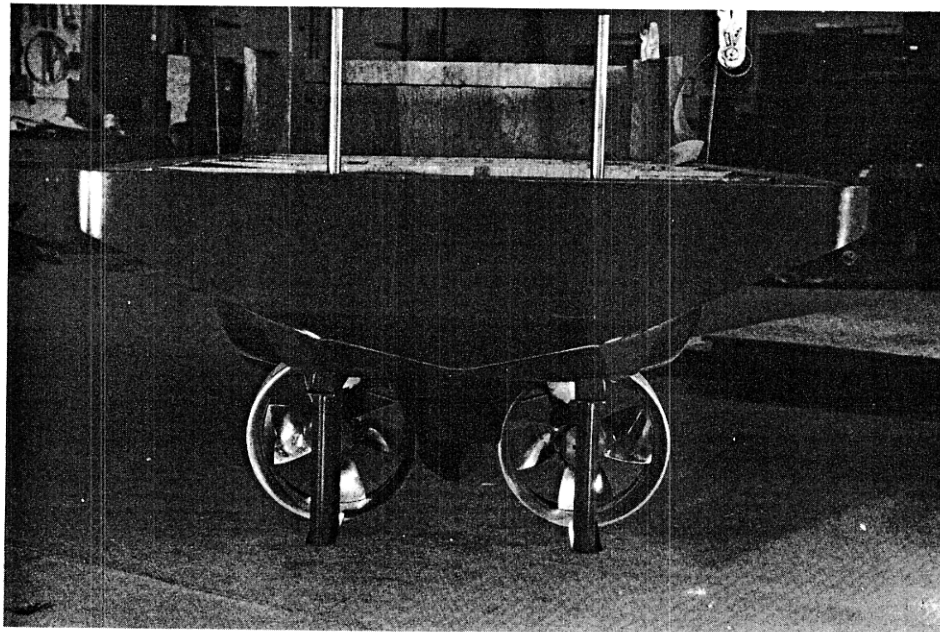
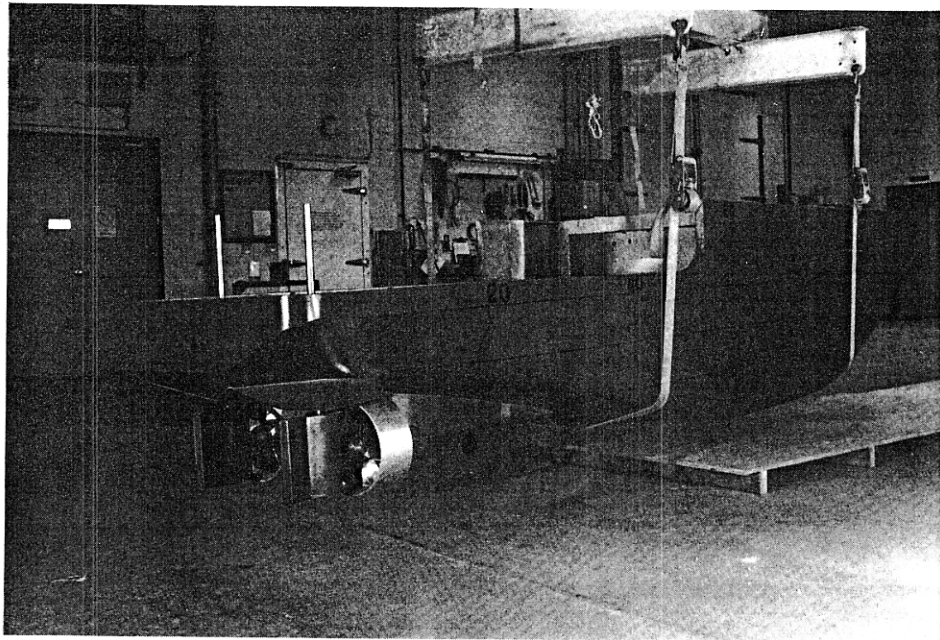
Figure 6. Model of Antarctic research vessel.

strength for the first three sheets only. The results of the measurements are listed in Table 2. These measurements confirm past experience at CRREL that the ratio E/σ_f is of the order of 1500 in the average and that the strength ratio σ_c/σ_f varies between 3 and 4.5.

In the fourth and thickest sheet, the ice flexural strength at the 6-m mark along the test basin was measured at 43 kPa and the ramming tests were initiated. However, the strength was measured again at the 16-m mark about halfway in the test program, and at the 28-

Table 2. Measured ice sheet properties.

Sheet no.	h_i (mm)	σ_f (kPa)	E (MPa)	σ_c (kPa)	E/σ_f	σ_c/σ_f
1	55 ±2	44 ±2	60	100 ±30	1350	3.65
2	30 ±1	42 ±4	77	190 ±40	1800	4.50
3	52 ±2	41 ±3	48	136 ±15	1170	3.32
4	95 ±3	43 to 50	—	—	—	—



b. Hull with appendages and propellers.

Figure 6 (cont'd).

m mark at the end of the tests. In both cases the average flexural strength was found to be 50 kPa, i.e., 25% greater than expected.

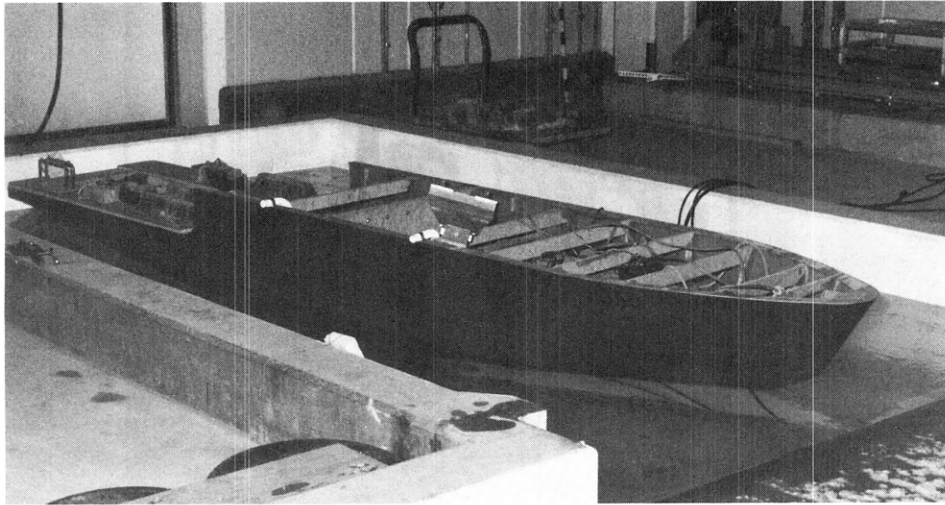
EXPERIMENTAL SET-UP

Ship model

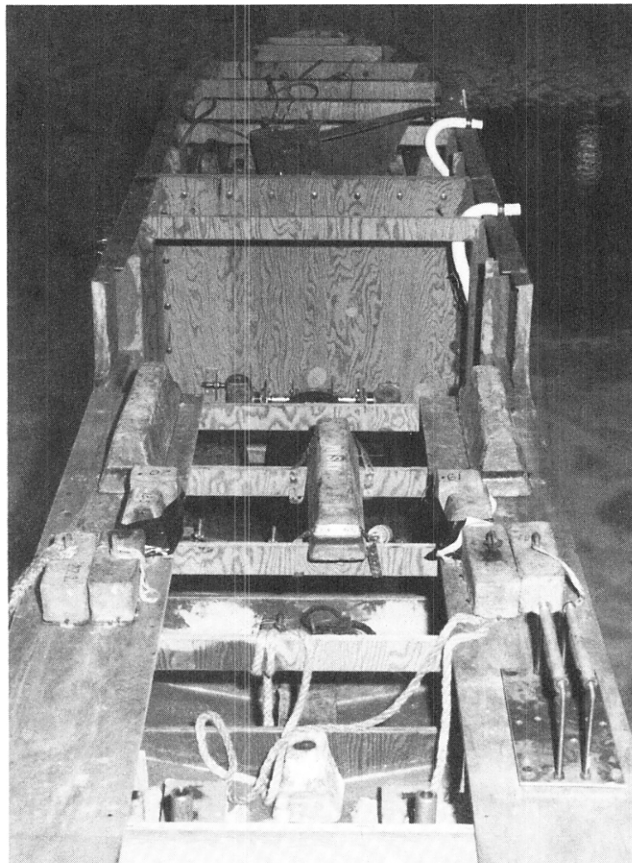
The ship model and all appendages were delivered to CRREL and assembled by personnel from Offshore Research, Ltd., the technical monitor of the model tests

program for North American Shipbuilding, Inc. (Fig. 6).

The initial resistance tests in level ice were to be conducted with the naked hull. The model, without the appendages, was ballasted in the trim tank of the CRREL ice towing tank. Ballast was so distributed as to match the required draft, and to closely approximate the required *GM* of 7.5 cm. Incline tests were made and, after several adjustments in the ballast distribution, the actual model *GM* was measured to be 8.0 cm and considered



a. Side view.



b. Top view.

Figure 7. Ballasted model in trim tank.

to be sufficiently close to the required value. Photographs of the ballasted model in the trim tank are shown in Figure 7.

The model roll period was measured at 3.15 seconds, which corresponds to 13.4 seconds at full scale. When all the appendages were added prior to the propulsion tests, the roll period was measured at 2.85 seconds or 12.2 seconds at full scale.

In both resistance and captive-model propulsion

tests, the ship model was connected to the towing carriage by a $1\frac{1}{2}$ -in. (3.8-mm) towing post that could slide vertically in a linear ball-bearing. The tow post was attached to a double-gimbal mounted on a force block that was bolted to the bottom of the model. The pivot point of the double-gimbal was located in alignment with the model shaft line at frame 84, i.e., slightly forward from midship.

The ship model was thus free to heave, pitch and roll

but was totally restrained in surge and sway. It was restricted in yaw by a fork mounted on the stern of the model and straddling a vertical rod attached to the carriage. As seen in Figure 7a, this fork was mounted on the starboard side of the stern. By imparting a roll to the model, the positive yaw control system was checked and found to not affect the roll motion significantly. Furthermore, the roll during the model tests in ice was of very small amplitude, if at all noticeable.

For the propulsion tests, the model was equipped with two thrust-and-torque dynamometers, one per propeller shaft. Both shafts were driven by a single 3-hp (2.3-W) variable-speed electric dc motor (FINCOR Model 9230018TFB) with a controller (FINCOR Model 2453B300) that was equipped with a tachometer servo-mechanism to maintain the rotational speed at the set value.

Measurement transducers

The model resistance during resistance tests or pull during propulsion tests was measured by a 500-lb (2200-N) capacity force block (Tracor-Hydronautics Model HI-M-4) that had its own power supply and signal conditioner. The thrust and torque on each propeller shaft were measured by a Sensor Developments, Inc., dynamometer (model no. 22001-251-012) rated at 250 lb (1100 N) in thrust and 100 in. lb (11 N m) in torque.

All these transducers were calibrated statically prior to the tests over the expected range of force and torque. Repeatability in the calibration indicated that the force

block and the thrust sensors were accurate to ± 2 N (± 0.5 lb), while the torque sensors were accurate to ± 0.05 N m (± 0.5 in. lb).

The rotational speed of the propellers was measured by a magnetic pickup mounted over a 60-tooth gear fastened to one of the propeller shafts. The frequency of the magnetic pickup was converted to a dc voltage by a frequency-to-voltage converter for digital sampling by the data acquisition system. The accuracy of the rpm measurements was ± 1 rpm.

Data acquisition system

The data acquisition system consisted of a NEFF 620, made of a Model 100 power supply and signal conditioner and a Model 300 signal processor (analog-to-digital converter), controlled by an HP-9845B desktop computer (Fig. 8).

The carriage speed, force block output and rpm counter voltage were all filtered by 10-Hz filters and amplified with a gain of 10 (the minimum NEFF gain). The thrust signals from the dynamometers were amplified with a gain of 500, the torque signals with a gain of 1000. All signals were scanned at the same rate, which varied from 200 to 100 Hz, depending upon the test, i.e., the sampling interval varied between 5 and 10 ms. The data in digitized form were stored on floppy disks for subsequent analysis.

Video and photographic coverage

The tests were recorded both on still color photo-

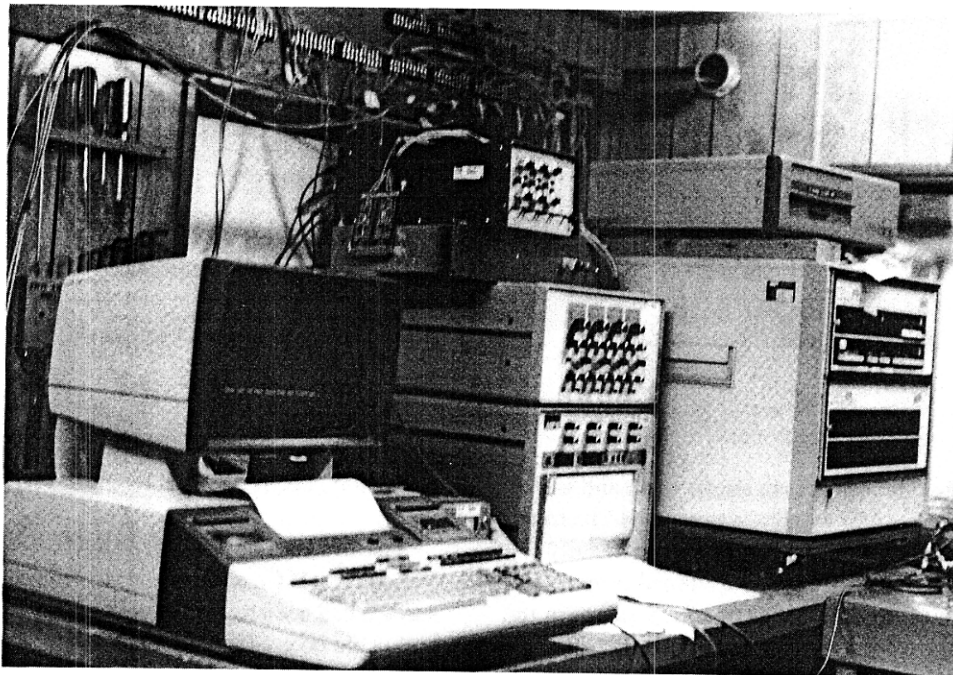
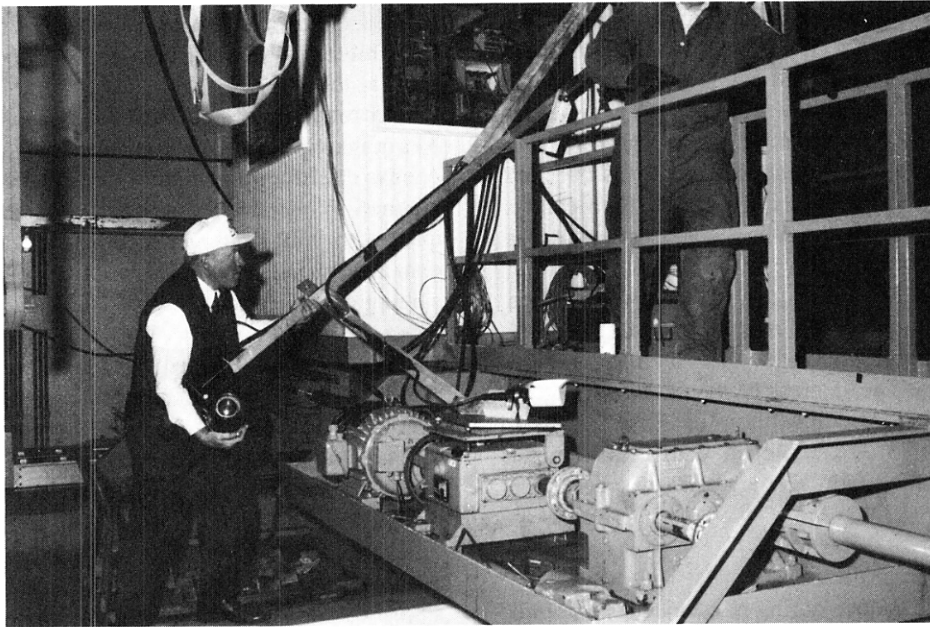
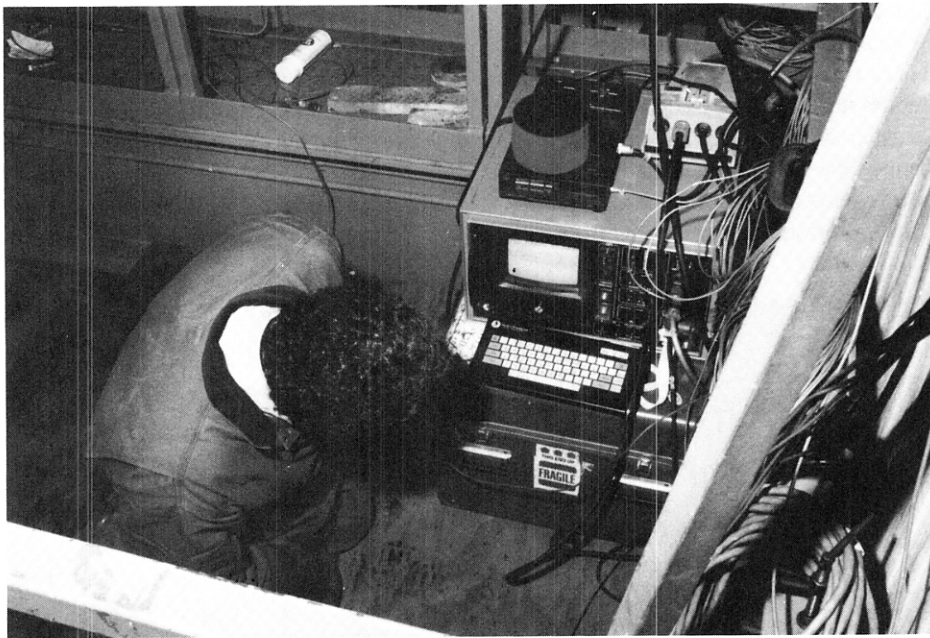


Figure 8. Data acquisition system.



a. Video camera and support.



b. Controls.

Figure 9. Underwater video system.

graphs and on video tapes both above water and underwater. The underwater camera was mounted from the back of the carriage and suspended approximately 6 ft (1.8 m) underwater (Fig. 9). It was aimed primarily at the stern area to observe the flow of ice pieces in the vicinity of the propellers and nozzles. All original videos were forwarded to North American Shipbuilding, Inc., at the conclusion of the model tests.

ICE FRICTION TESTS

The model manufacturer, Offshore Research Ltd., Vancouver, B.C., also provided a friction board whose surface had been treated in the same manner as the ship hull. This board was mounted on the CRREL friction table (Fig. 10), with an ice sample held in place on the board by a sample holder connected at both ends to a

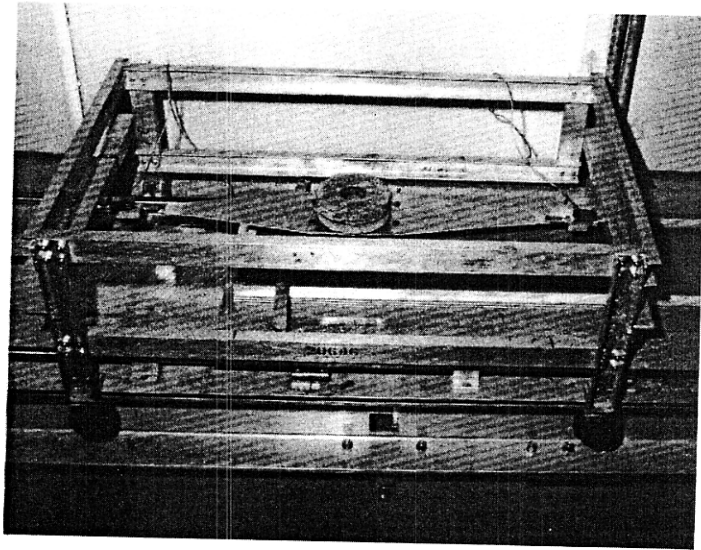


Figure 10. Friction table.

Table 3. Results of ice friction tests.

Test no.	F_N (N)	F_T (N)
Series 1		
801	36.2	3.70
802	58.5	5.90
803	80.5	7.30
804	109.9	8.50
Series 2		
805	107.7	7.30
806	63.2	4.80
807	85.3	5.80
808	40.8	3.00

load cell (10-lb [45-N] capacity). An additional weight, from 5 to 20 lb (22 to 89 N), was added on top of the sample holder. The friction table is set in motion and the frictional force measured by the load cells was recorded via the NEFF data acquisition system over two back-and-forth cycles of the table. Two series of friction tests were made on two consecutive days. All tests were

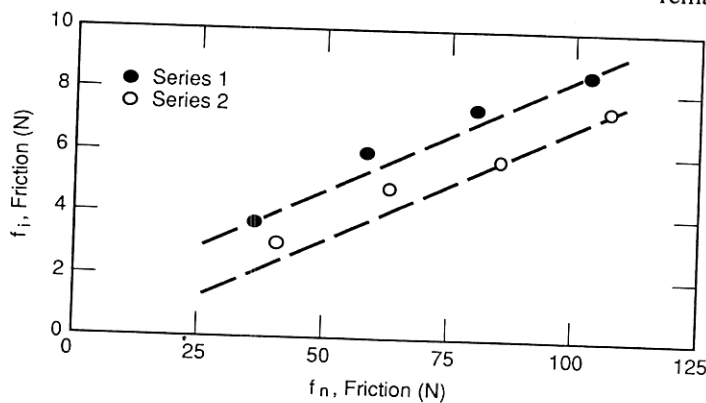


Figure 11. Results of friction tests.

made at a speed of 15 cm/s. The test results are listed in Table 3 and shown graphically in Figure 11.

The friction factor f_i is defined as the slope of the tangential force F_T versus normal load F_N (Tatinclaux 1989). The two test series yielded nearly the same slope, namely $f_i = 0.074$.

RESISTANCE TESTS IN LEVEL ICE

General

Ice resistance tests were made in two ice sheets. The target thicknesses were 50 and 25 mm to simulate full-scale ice thicknesses of 3 and 1.5 ft respectively. The target model flexural strength was 38 kPa (5.5 lb/in.²), corresponding to the full-scale value of 700 kPa (100 lb/in.²). The actual ice thickness and strength of the first model ice sheet were 55 mm and 44 ± 4 kPa, respectively, and those of the second ice sheet were 30 mm and 40 ± 3 kPa respectively (Table 2).

Test procedure

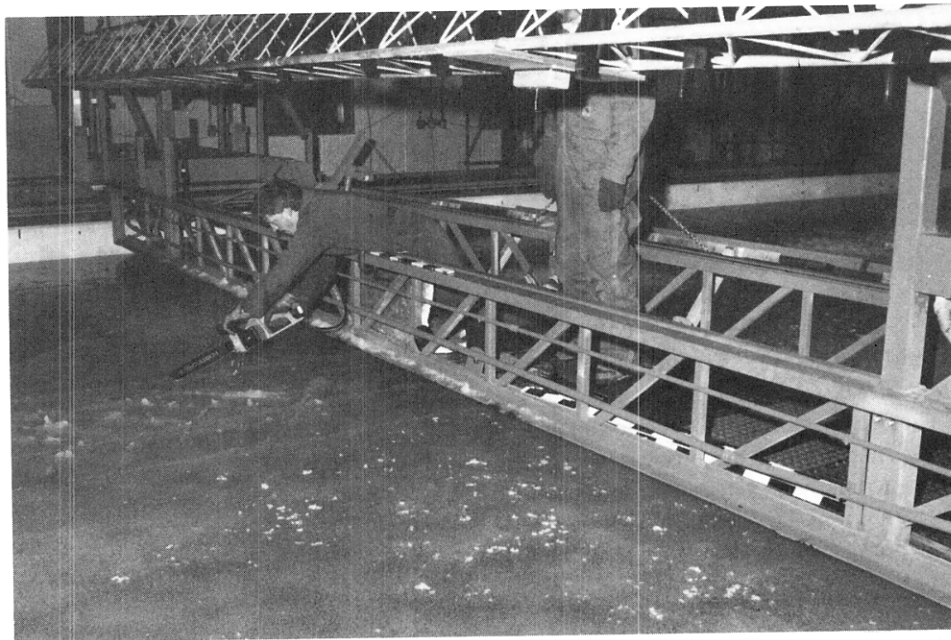
Three tests at three different ship speeds were made in each ice sheet over distances of 10 to 12 m. The ice length for each test was composed of a sawn ice channel and of a solid, intact section. The sawn sections were cut in a chevron pattern (Fig. 12 and 13) to simulate the icebreaking pattern. The sawn width was 1.20 m, i.e., 20% wider than the model's beam. This ensured that pieces of ice did not get trapped and crushed between the model hull and the edge of the surrounding sheet ice.

For each test, the length of the intact ice section was at least 5 m to ensure that the ship model would penetrate at least one full length into level ice. This distance was deemed sufficient to obtain a reliable average of the ice resistance over one-half to three-quarters of a ship length, since the maximum resistance is usually achieved when the ship shoulders have penetrated the ice. The remainder of the ship body contributes little if any additional resistance, especially for a hull with relatively sharp shoulders such as the one being tested.

In both ice sheets, the first test was made at the lowest required speed, the second test at the highest speed and the third at the intermediate speed. Prior to the second and third test, the ship model was backed into the pre-viously broken channel to allow sufficient distance for the carriage to reach steady speed before entering the sawn channel on the following run. In some cases, it was possible to obtain also a measurement of the model resistance in ice-free, open water.



a. Longitudinal cuts.



b. Chevron pattern.

Figure 12. Sawing the channel.

Observation and data presentation

A view of the breaking pattern at the bow is presented in Figure 14, which shows the typical herring bone pattern. Figure 15 shows a typical example of the channel created by the ship model during the resistance tests. It is worth mentioning that the channel was relatively free of ice, and that most of the ice floes broken by the hull had been pushed aside underneath the surrounding

level ice. This was confirmed by underwater observations that also showed that little ice reached the stern area.

Time histories of the recorded carriage speed and model resistance are plotted on Figure 16a for the tests in the 55-mm ice sheet and in Figure 16b for those in the 30-mm ice sheet. Also shown are the record lengths over which data were averaged to obtain resistance in

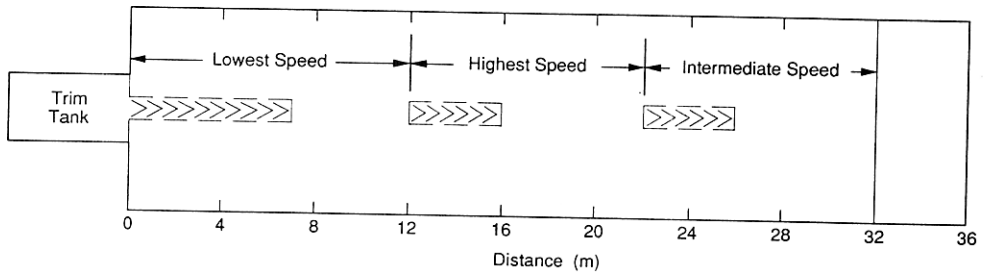
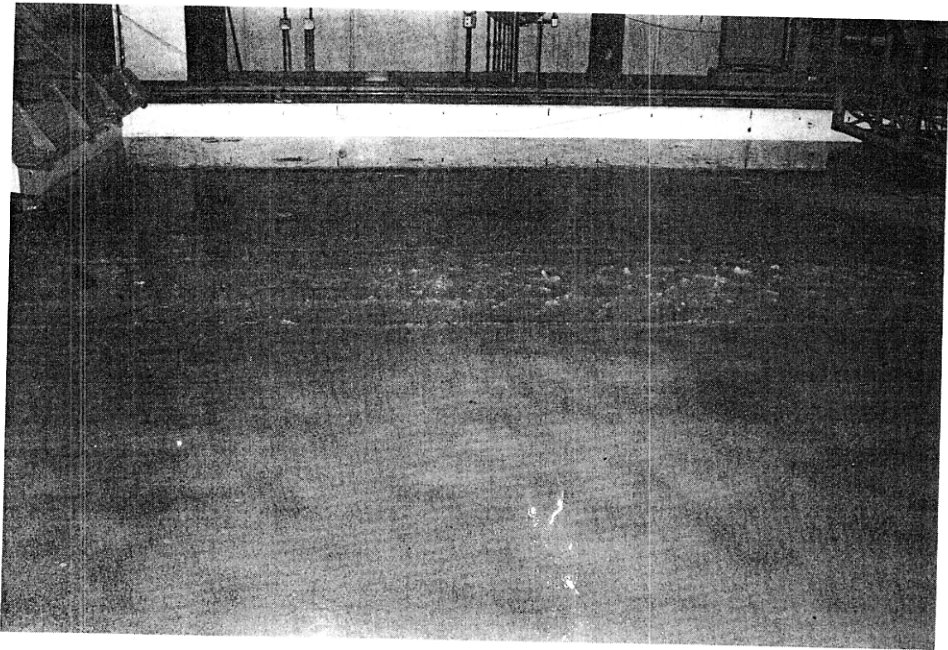


Figure 13. Sawn channel and general layout.

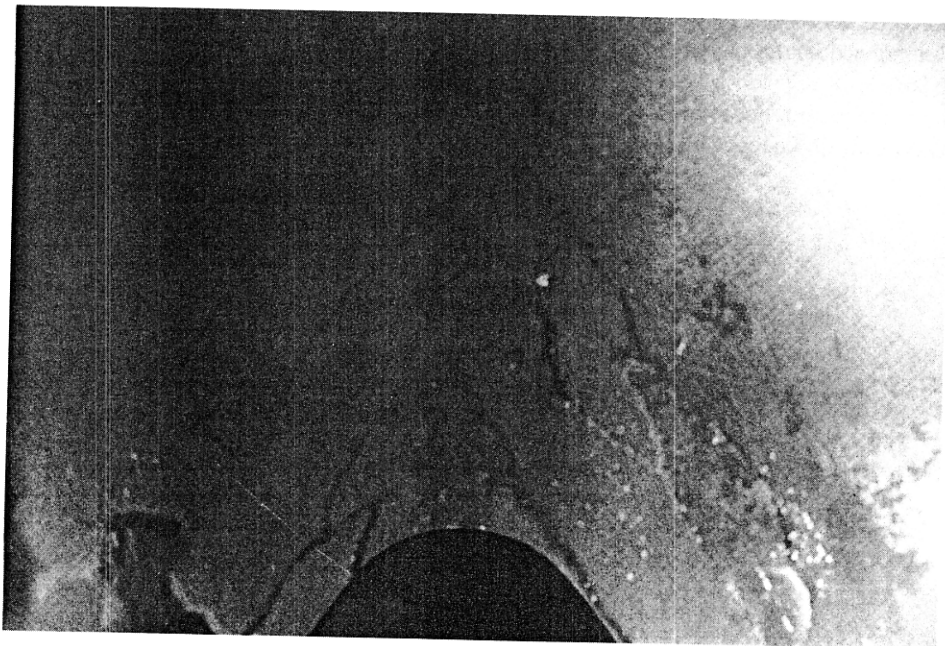


Figure 14. Breaking pattern at model bow.

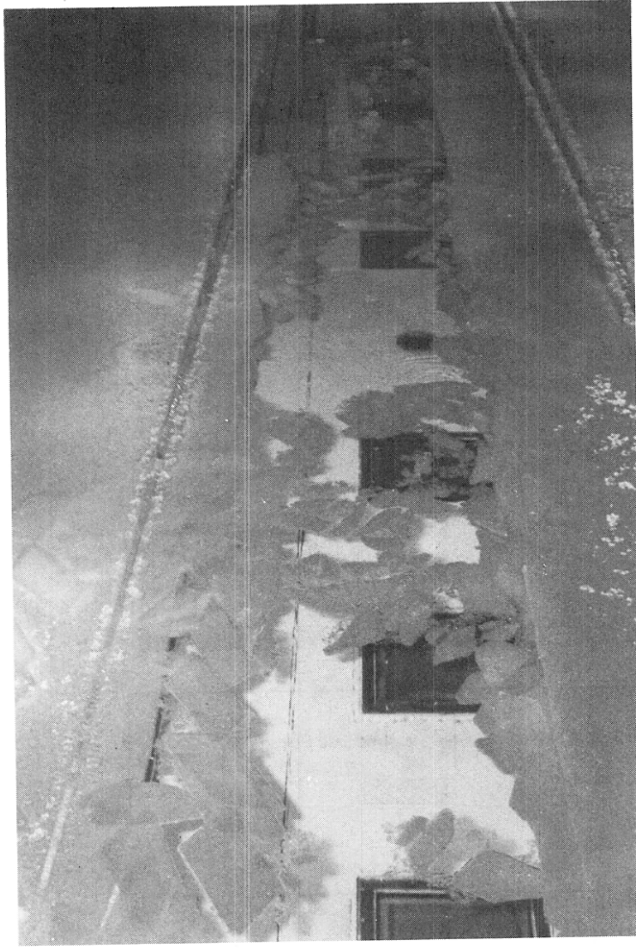


Figure 15. Channel behind ship model during resistance tests.

sawn ice, R_{ps} and total ice resistance R_{it} . In particular, R_{it} was usually averaged over one-half to three-quarters of a model ship length.

Table 4 lists the measured values of R_{ps} and R_{it} , as well as the viscous or frictional resistance R_f calculated by

$$R_f = C_F \frac{1}{2} \rho S V^2 \quad (3)$$

where ρ = water density

V = ship speed

S = wetted area

C_F = friction coefficient given by the ITTC 57 formula.

In addition Table 4 lists the submergence resistance R_s and the breaking resistance R_{bk} defined by

$$R_s = R_{ps} - R_f \quad (4)$$

$$R_{bk} = R_{it} - R_{ps} \quad (5)$$

Table 4 also lists the corresponding adimensional quantities.

Data analysis

The component R_s is interpreted as the net ice resistance at zero flexural strength (Colbourne 1989). When made non-dimensional by $\gamma B h_i$, where γ = specific gravity of water, B = ship beam, and h_i = ice thickness, it is to be only a function of the Froude number based on ice thickness $F_n = V/\sqrt{g h_i}$, as indeed shown in Figure 17.

On the other hand, the non-dimensional breaking resistance, $R_{bk}/\gamma B h_i$, is shown to be independent of F_n (Fig. 18a) but to be a linear function of the strength coefficient $C_n = \sigma_f/\gamma h_i$ in Figure 18b.

Linear regression of the data in Figures 17 and 18b yielded

$$\frac{R_s}{\gamma B h_i^2} = 3.32 \frac{V}{\sqrt{g h_i}} \quad (6)$$

and

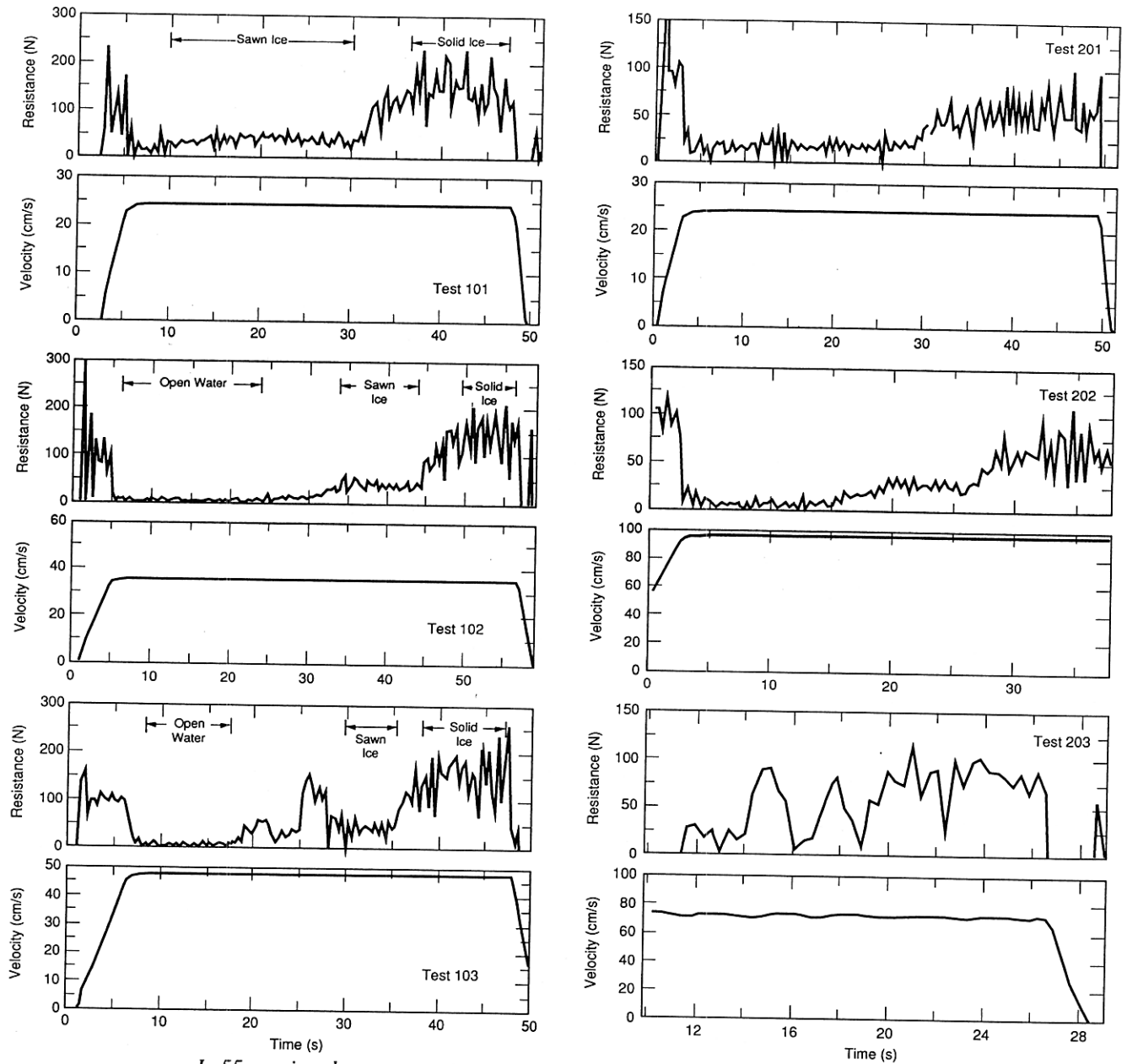
$$\frac{R_{bk}}{\gamma B h_i^2} = 3 + 0.0075 \frac{\sigma_f}{\gamma h_i} \quad (7)$$

Full-scale resistance predictions

Full-scale predictions of the resistance in ice of

Table 4. Results of resistance tests in level ice.

Test no.	Dimensional data						Nondimensional data			
	V (cm/s)	R_{ps} (N)	R_{it} (N)	R_f (N)	R_s (N)	R_{bk} (N)	F_n	$\sigma_f/\gamma h_i$	$R_s/\gamma B h_i^2$	$R_{bk}/\gamma B h_i^2$
$h_i = 55 \text{ mm}; \sigma_f = 44 \text{ kPa}$										
101	24.2	36.2	143.5	0.8	35.4	107.3	0.33	81.5	1.19	3.59
102	35.7	39.3	148.3	1.6	37.7	109.0	0.49	81.5	1.26	3.65
103	47.5	50.2	158.0	2.6	47.6	107.0	0.65	81.5	1.59	3.61
$h_i = 30 \text{ mm}; \sigma_f = 40 \text{ kPa}$										
201	24.2	17.8	56.3	0.8	17.0	38.5	0.45	135.9	1.92	4.33
202	48.2	27.5	61.4	2.7	24.8	33.9	0.89	135.9	2.79	3.82
203	72.6	48.1	83.0	5.6	42.5	34.9	1.34	135.9	4.79	3.93



a. In 55-mm ice sheet.

b. In 30-mm ice sheet.

Figure 16. Records of resistance tests.

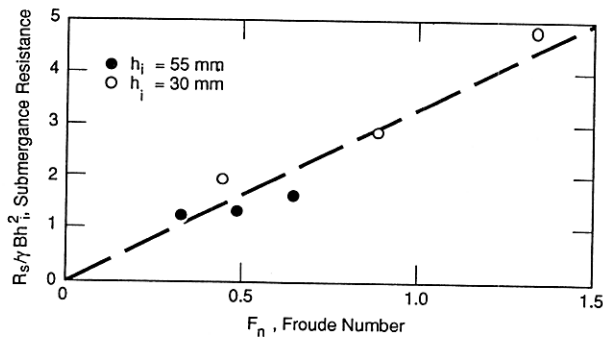


Figure 17. Nondimensional submergence resistance vs. Froude number.

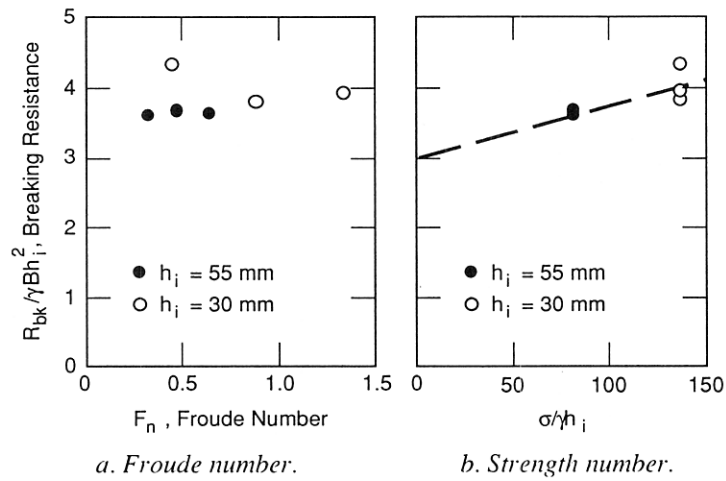


Figure 18. Nondimensional breaking resistance vs two parameters.

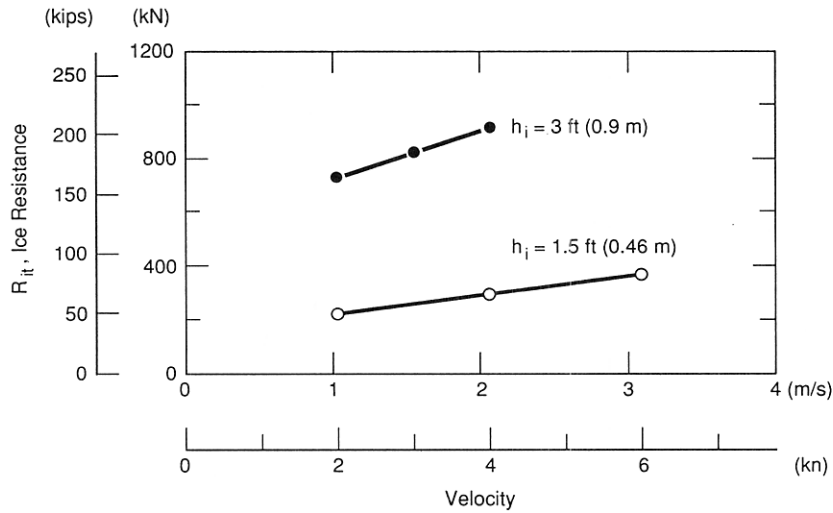


Figure 19. Predicted full-scale ice resistance of naked hull.

the naked hull can be made on the basis of eq 3–7. At full scale it is customary to increase the coefficient C_F given by the ITTC 57 formula by a so-called roughness allowance, usually of the order of 0.0004. Then, the full-scale total ice resistance is given by

$$R_{it} = (C_f + 0.0004) \frac{1}{2} \rho S V^2 + \gamma B h_i^2 (3 + 3.32 F_n + 0.0075 C_n). \quad (8)$$

Calculated values are presented graphically in Figure 19, and listed in Table 5 where $R_i = R_s + R_{bk}$.

RESISTANCE TESTS IN OPEN WATER

To complement the model resistance tests in level ice, a series of resistance tests in ice-free or open water

was conducted both with the naked hull and after all appendages, including the nozzles, had been mounted but without the propellers.

Table 5. Predicted full-scale resistance of naked hull.

V (kn)	R _f (kN)	R _i (kN)	R _{it} (kN)
h_i = 3 ft			
2	3.2	725	728
3	6.8	813	820
4	11.7	901	913
h_i = 1.5 ft			
2	3.2	221	224
4	11.7	283	295
6	25.0	346	371

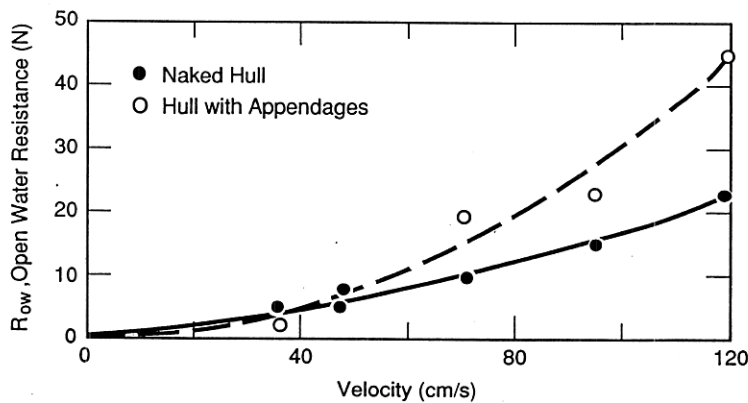


Figure 20. Results of resistance tests in open water.

The results of these tests are listed in Table 6 and shown graphically in Figure 20.

It should be noted that at the model velocity of 36 cm/s, corresponding to 3 kn (0.9 m/s) at full scale, the open water model resistance is of the order of the accuracy of the force block measurements (i.e., 2 N) both with and without appendages. A second-order polynomial regression analysis gave the following equations

$$\text{Naked hull: } R_{ow}(N) = V(8 + 9V) \quad (9)$$

$$(r = 0.992)$$

$$\text{Hull with appendages: } R_{ow}(N) = V(-0.28 + 31V) \quad (10)$$

$$(r = 0.978)$$

where V is expressed in meters/second and r is the regression coefficient. Therefore, the added resistance due to the appendages can be expressed by

$$R_{app}(N) = V(22V - 8.3). \quad (11)$$

This last equation is valid only for the range of velocity $0.4 < V < 1.2$ m/s.

There is no universally accepted way of extrapolating appendage resistance to full-scale conditions. Because the Reynolds number of the model appendages is much smaller than at full scale, the added resistance of the appendages at model scale will be relatively much greater than at full scale.

It can be suggested that the full-scale appendage resistance may be estimated as half the model appendage resistance extrapolated by λ^3 . Thus, the full-scale appendage resistance for the present hull can be expressed by

$$R_{app}(kN) = V(3.64V - 5.85) \text{ at full scale} \quad (12)$$

with V expressed in meters/second; eq 13 is valid for $1.7 < V < 5.1$ m/s, approximately.

Table 6. Results of open-water resistance tests.

Test no.	V (cm/s)	R_{ow} (N)
Naked hull		
10	71.1	9.8
11	95.0	14.9
12	118.8	22.8
102	35.7	4.6
103	47.5	5.0
202	48.2	7.3
Hull with appendages		
13	36.3	2.4
14	70.5	19.4
15	94.7	23.2
16	119.2	44.9

OVERLOAD PROPULSION TESTS IN OPEN WATER

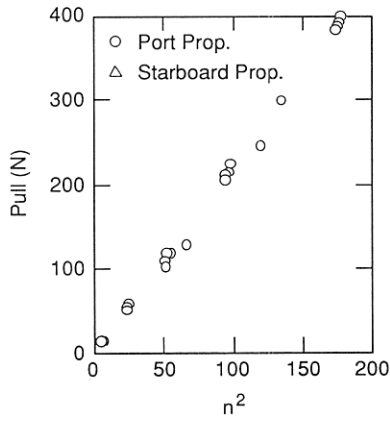
General

Overload propulsion tests over a range of propeller speeds from 150 to 800 rpm, approximately, were conducted at three model speeds corresponding to full-scale ship speed of 3, 6 and 8 kn (1.5, 3.1 and 4.1 m/s) respectively. In addition, at the start of some of the propulsion tests in level ice described in a subsequent section, the ship model traveled in an ice-free channel during which measurements were also taken.

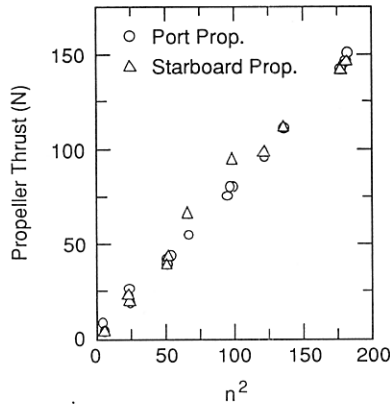
A series of bollard tests (i.e., overload tests at zero speed) was also made over the above range of propeller speeds (test no. 920). Measurements under bollard conditions were usually made at the beginning of the overload tests and propulsion tests both in open water and in ice.

Data presentation and analysis

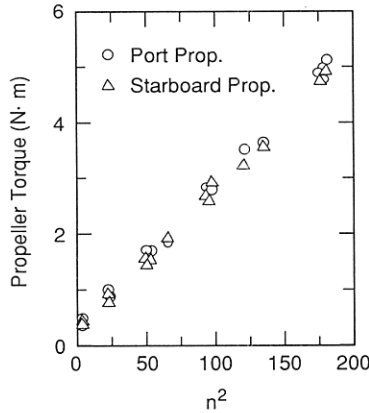
The results of all bollard tests are listed in Table 7 and shown graphically in Figure 21. From Figure 21, it can



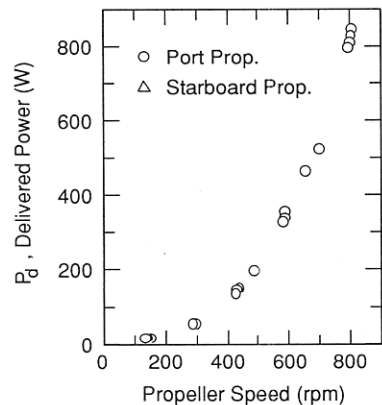
a. Pull vs n^2 .



b. Propeller thrust vs n^2 .



c. Propeller torque vs n^2 .



d. Delivered power vs propeller speed.

Figure 21. Results of bollard tests.

Table 7. Results of bollard tests.

rpm	Pull (N)	Thrust (N)		Torque (N m)		P_d (W)
		Port	Starboard	Port	Starboard	
Bollard test 920						
141	11.3	7.5	4.3	0.44	0.44	13
291	49.7	20.9	18.2	0.95	0.90	56
429	109.8	39.5	39.9	1.66	1.55	144
584	206.0	75.5	75.0	2.79	2.65	333
807	397.5	151.3	145.8	5.07	4.90	843
Overload tests						
146	12.6	4.5	4.8	0.37	0.38	11
150	12.7	4.1	4.2	0.36	0.41	12
293	50.9	26.0	21.9	0.93	0.77	52
297	52.4	19.5	19.6	0.87	0.80	52
300	56.2	18.5	19.1	0.84	0.82	52
431	104.5	42.6	39.1	1.64	1.41	138
439	116.5	41.9	41.9	1.64	1.53	146
444	117.9	43.1	41.9	1.67	1.51	148
588	210.0	79.4	79.5	2.77	2.59	330
593	212.2	79.6	77.5	2.75	2.64	335
660	243.9	96.0	97.6	3.46	3.20	461
796	381.7	142.4	141.5	4.84	4.73	798
799	385.1	142.8	141.9	4.89	4.72	804
803	392.6	146.5	143.4	4.97	4.77	819
Propulsion tests in ice						
490	128.7	54.4	65.7	1.82	1.91	191
595	220.9	79.1	94.4	2.74	2.90	352
699	297.8	111.3	111.0	3.59	3.54	522

be seen that the total pull, the propeller thrust and the propeller torque were proportional to the square of the propeller speed, n , in revolution-per-second (rps), and, therefore, that the delivered power, P_d is proportional to n^3 , namely

$$\text{Pull(N)} = 2.166n^2 \quad (r = 0.999)$$

$$\text{Propeller thrust} = T_p(\text{N}) = 0.814n^2 \quad (r = 0.998)$$

$$\text{Propeller torque} = Q_p(\text{N m}) = 0.0276n^2 \quad (r = 0.995)$$

$$\text{Delivered power} = P_d(\text{W}) = 0.344n^3 \quad (r = 0.999).$$

The results of the overload tests in open water at the three speeds—3, 6 and 8 kn full-scale—are listed in Table 8 and shown in Figure 22a–c. It was found that the pull, propeller thrust and propeller torque were linear functions of the square of propeller speed, i.e., $Y = k n^2 - Y_0$. Results of regression analysis on these data are given in Table 9.

Propeller coefficients

From the results of all the propulsion tests, including the tests in level ice discussed in the following section,

Table 8. Results of overload tests.

rpm	Pull (N)	Propeller thrust (N)		Propeller torque (N m)		P _d (W)
		Port	Starboard	Port	Starboard	
V = 3 kn full scale						
293	27.8	21.3	17.6	0.82	0.66	45
431	75.1	37.2	36.6	1.47	1.32	126
589	161.4	71.4	71.3	2.57	2.40	306
660	213.3	89.7	91.9	3.26	3.05	436
V = 6 kn full scale						
146	-26.4	-4.6	-4.4	0.12	0.14	4
297	-4.2	7.9	9.4	0.59	0.55	35
440	41.5	28.6	28.7	1.28	1.16	112
593	113.4	62.5	62.3	2.36	2.21	284
817	265.9	128.5	129.6	4.44	4.41	757
V = 8 kn full scale						
150	-44.4	-11.9	-11.5	-0.07	-0.03	-2
300	-25.2	1.0	1.8	0.42	0.40	26
444	5.8	22.1	22.6	1.13	1.00	99
597	78.8	54.5	54.8	2.18	2.04	264
818	225.0	121.0	121.3	4.28	4.16	723

Table 9. Results of regression analysis of overload test data ($y = kn^2 - Y_o$).

	Full scale					
	V = 3 kn		V = 6 kn		V = 8 kn	
	k	Y _o	k	Y _o	k	Y _o
Pull	1.91	-20	1.65	-43	1.52	-65
Thrust T _p	0.739	0	0.747	-10	0.741	-17.4
Torque Q _p	0.0124	0	0.0120	-0.0165	0.0119	-0.104

Note: In all cases the regression coefficient r was 0.999 or better.

the apparent advance coefficient $J = V/nD$ and the corresponding propeller coefficients, K_{TP} and K_Q , were calculated. The results are presented graphically in Figure 22d. In spite of the scatter, and on the basis of Figure 22d, a regression analysis of the data was made with the following results

$$K_{TP} = 0.329 - 0.371J^2 \quad (r = 0.997) \quad (14)$$

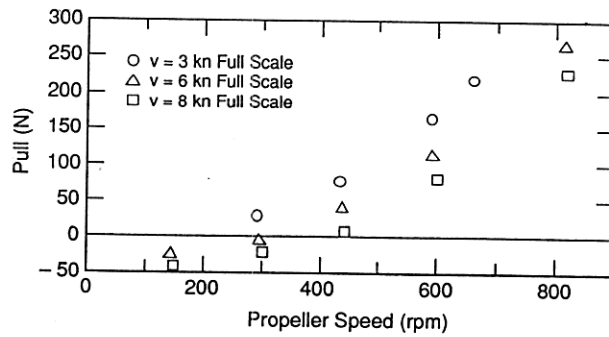
$$10K_Q = 0.508 - 0.179J^2 \quad (r = 0.975). \quad (15)$$

It should be noted that since the nozzles were not instrumented, it was not possible to measure the nozzle thrust and estimate the corresponding nozzle thrust coefficient. Neither was it possible to determine the overall thrust deduction factor.

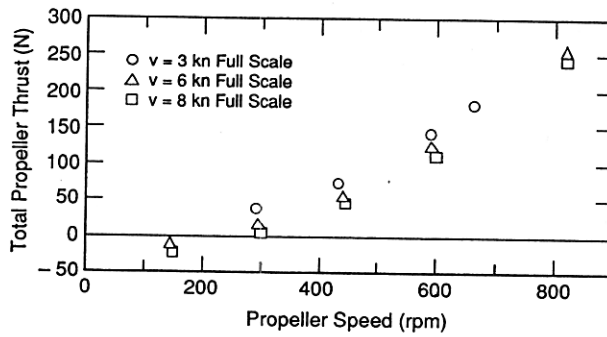
PROPULSION TESTS IN ICE

Test conditions and procedures

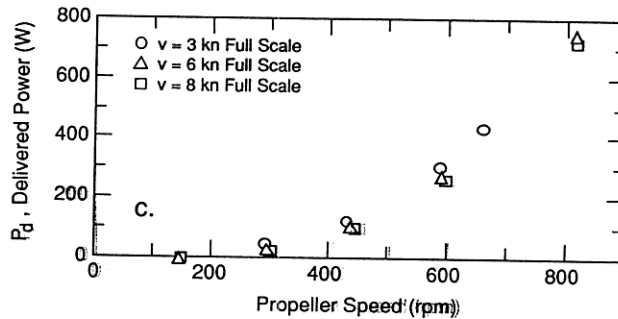
One ice sheet was devoted to propulsion tests with the captive model at one towing velocity of $V = 36 \text{ cm/s}$,



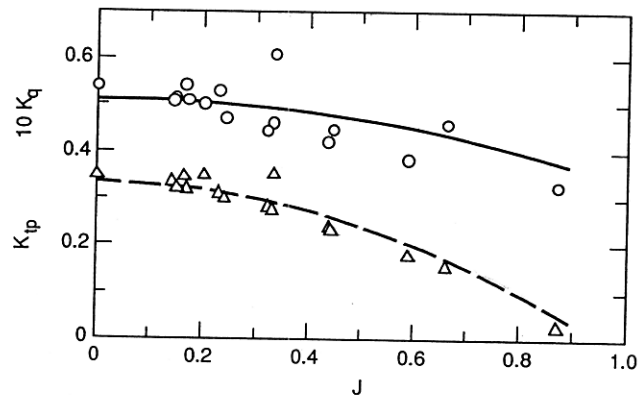
a. Pull vs propeller speed.



b. Total propeller thrust vs propeller speed.



c. Delivered power vs propeller speed.



d. Propeller coefficients.

Figure 22. Results of overload tests in open water.

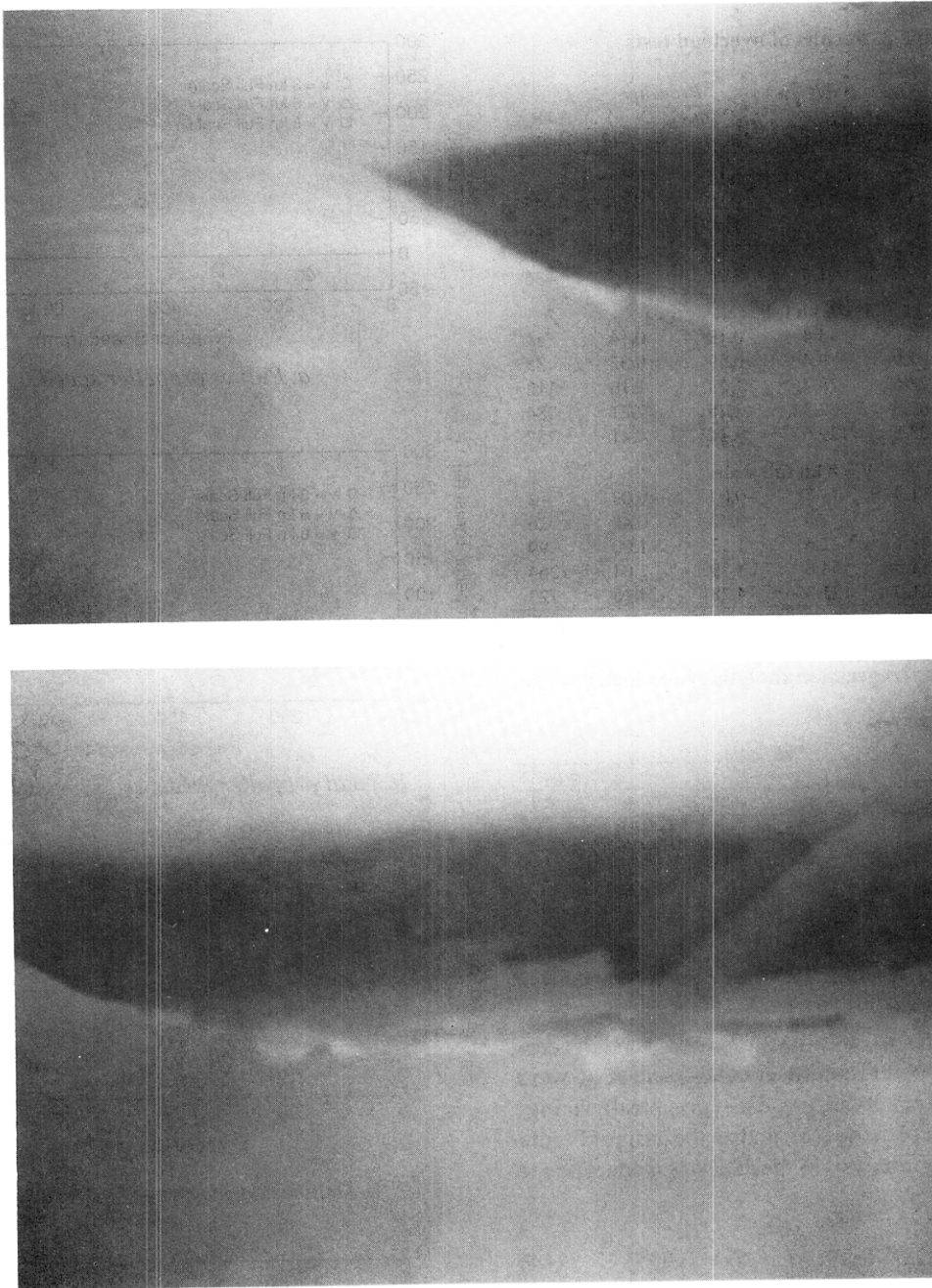


Figure 23. Underwater views during model propulsion tests.

corresponding to 3 kn (1.5 m/s) full scale. The full-scale ice thickness and ice strength to be modeled were 3 ft and 100 lb/in.² (0.9 m and 700 kPa), respectively, and the target model ice thickness and strength were 50 mm and 38 kPa, respectively. The actual ice sheet thickness was 52 ± 1 mm and the actual strength was 41 ± 3 kPa. Three tests at three propeller speeds were made, each over 10 more two-ship lengths, approximately. The first test was made at nearly 500 rpm, the second at nearly 600 rpm and the last at 700 rpm. These speeds were selected on the basis of the results of the ice resistance

and open water overload tests so that the model would be first underpropelled, nearly self-propelled and finally overpropelled.

As in the resistance tests, the carriage was stopped after each test, and backed a sufficient distance to allow in the subsequent test for model acceleration as well as some open water and ice-free conditions before the model entered the unbroken ice sheet.

Underwater views of the model during these tests are shown in Figure 23.

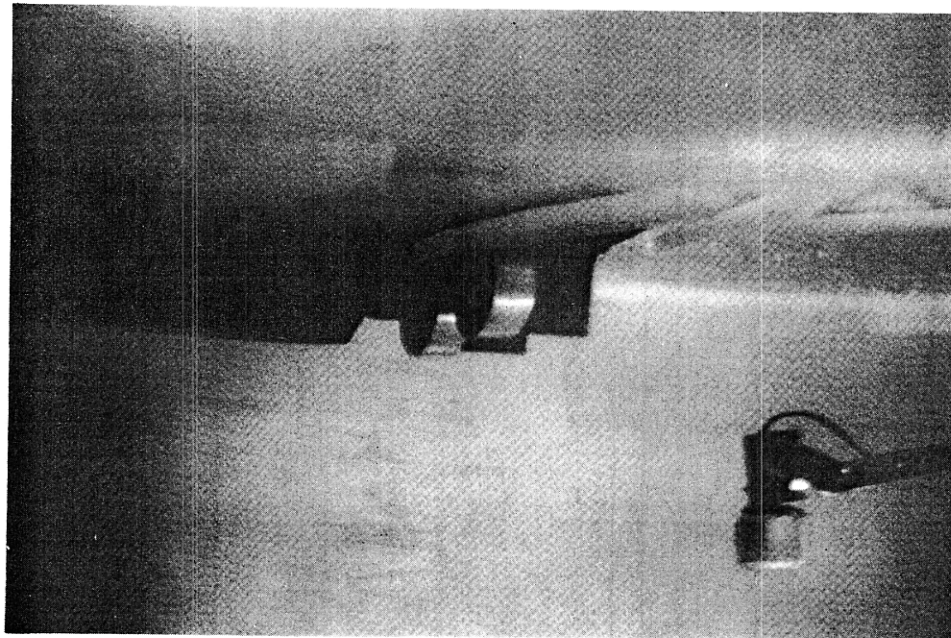
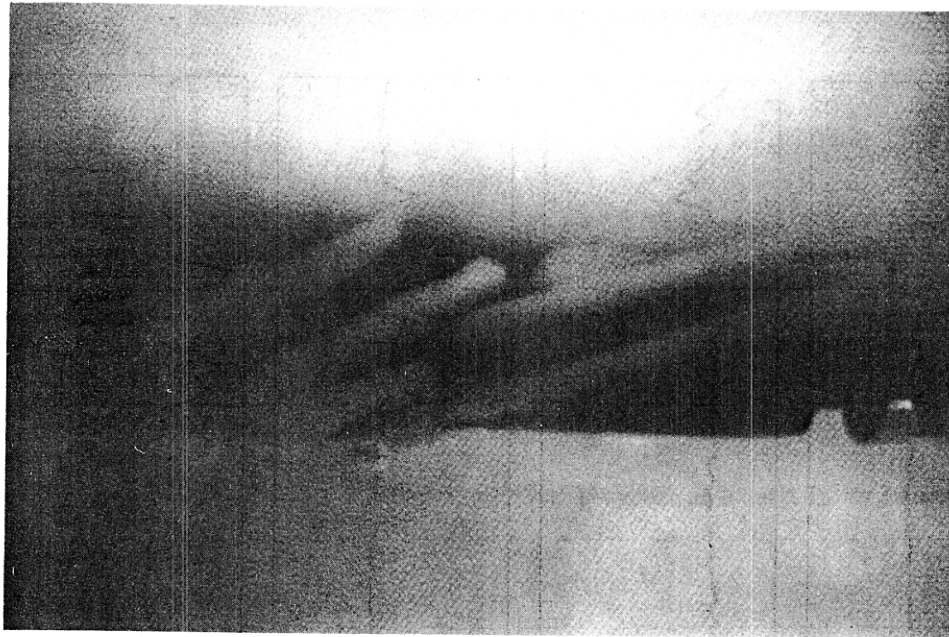


Figure 23 (cont'd).

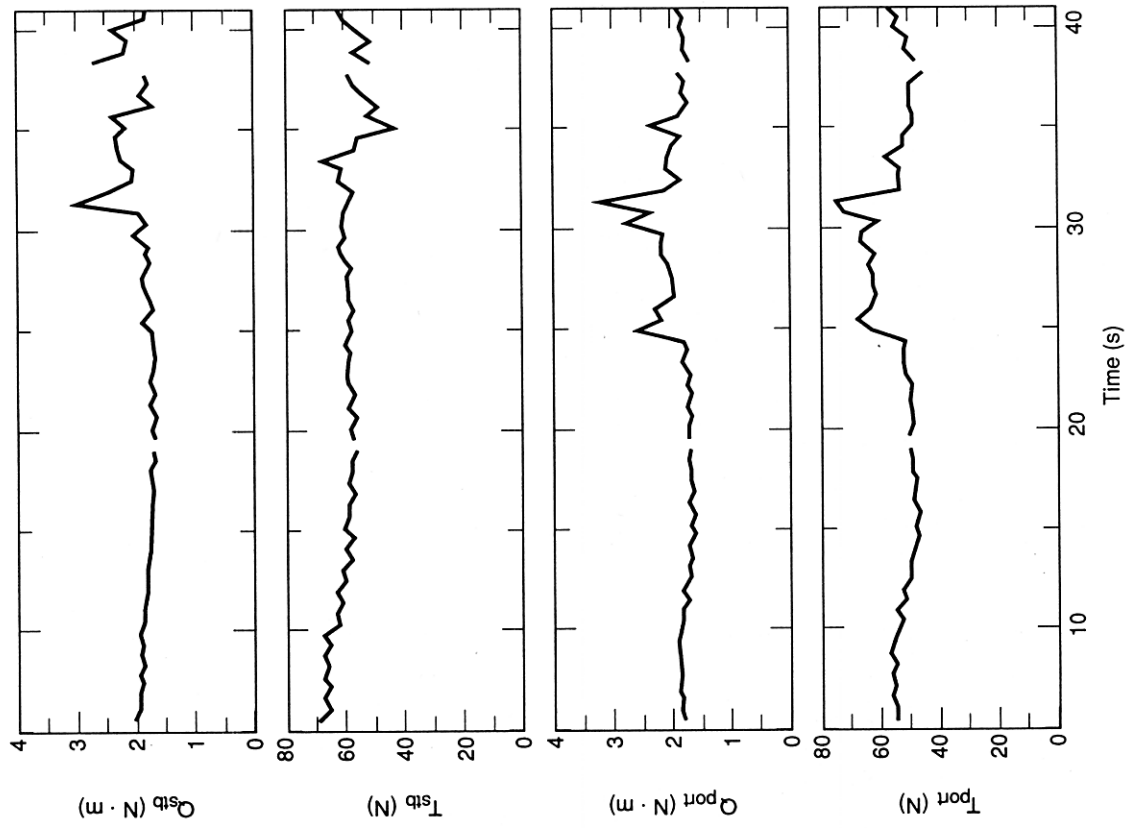
Data presentation and analysis

The time history of the force block and dynamometer outputs is shown in Figure 24 for all three tests. In all three tests, after the ship model has penetrated approximately one ship length into the ice, the thrust and the torque of one or both propellers exhibited irregularities, indicating that some ice was being entrained into the nozzles and interfering with the propellers. Such interference also appears to increase with increasing propeller speed.

Table 10 lists the average values of the total pull, propeller speed and propeller thrust and torque. Averages were made over those periods when there was no ice interference and when there was some ice-propeller interaction.

It can be noted that when there is entrainment of ice into the nozzle, both the propeller torque and the propeller thrust increase.

The test results without ice interference are plotted on Figure 25. The model self-propulsion point is the



a. Test 501.

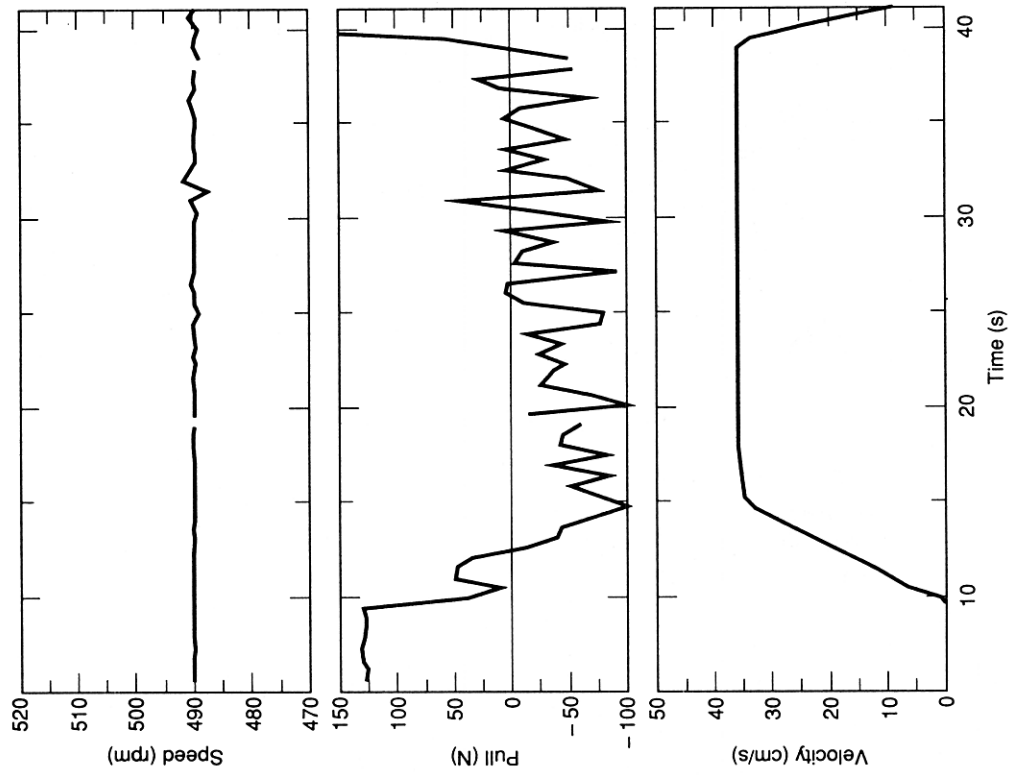
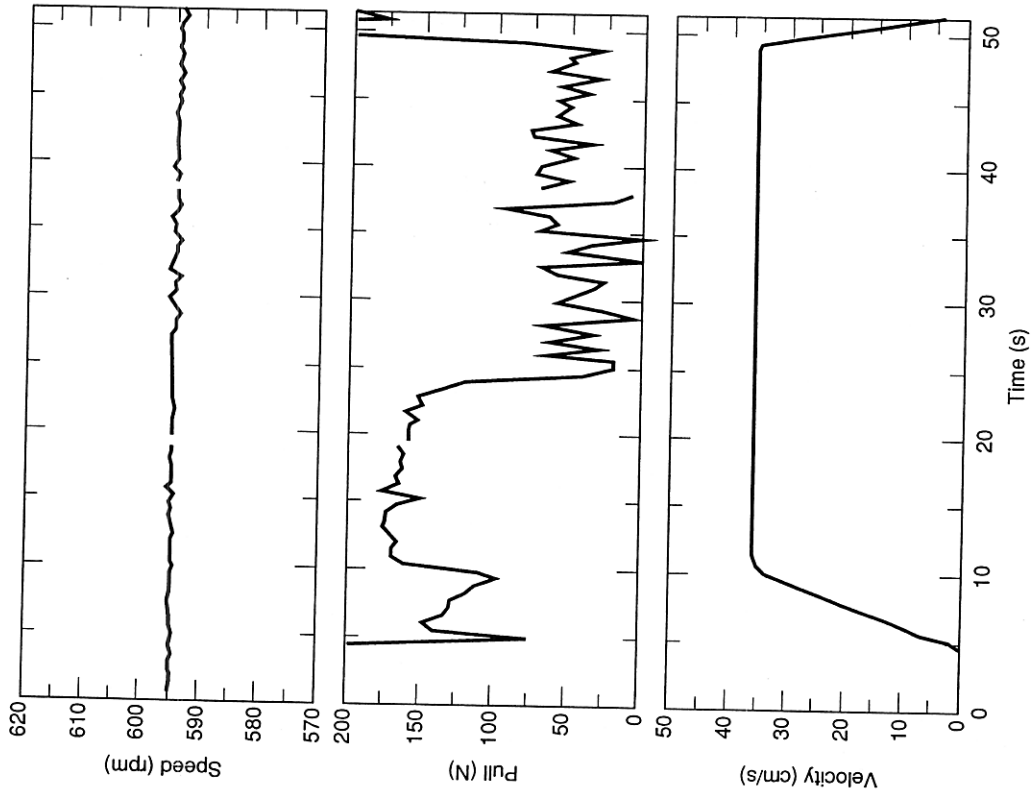
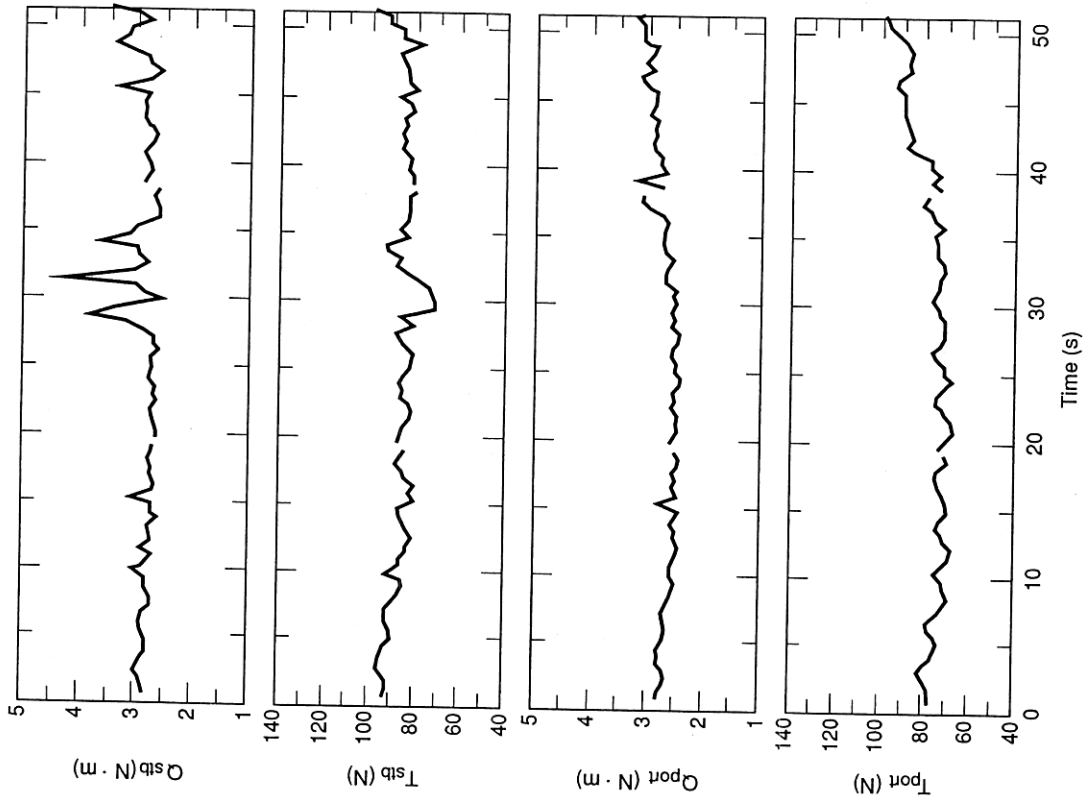
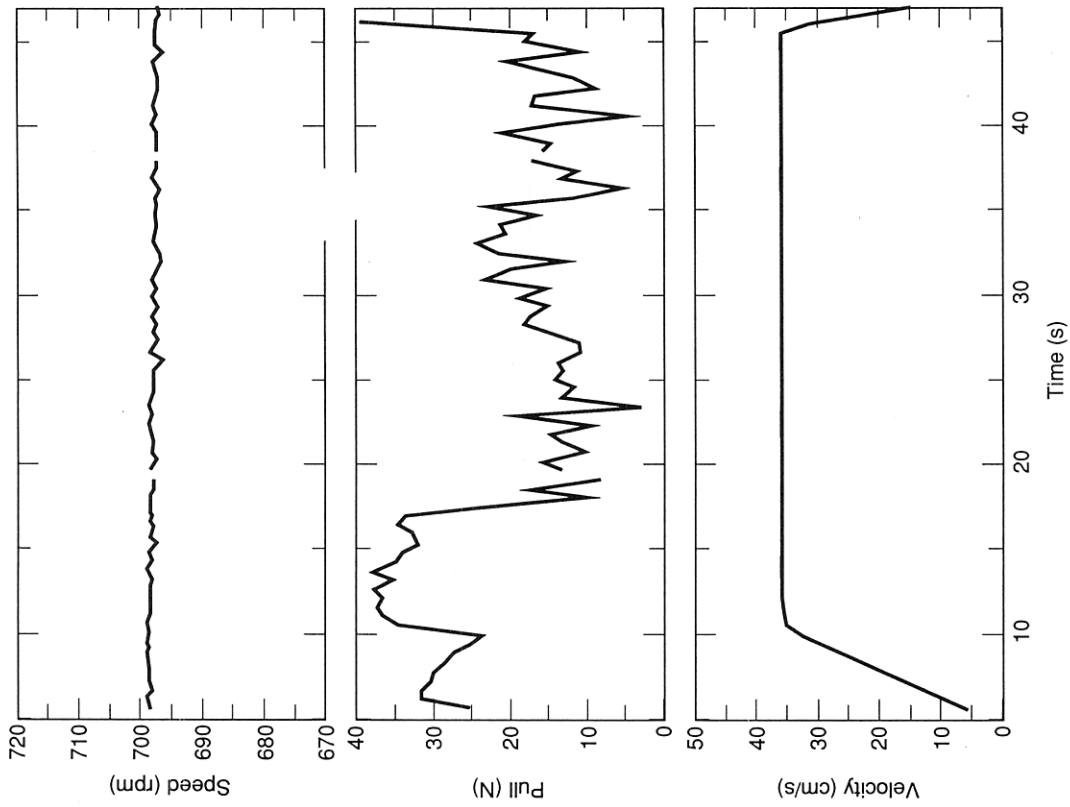
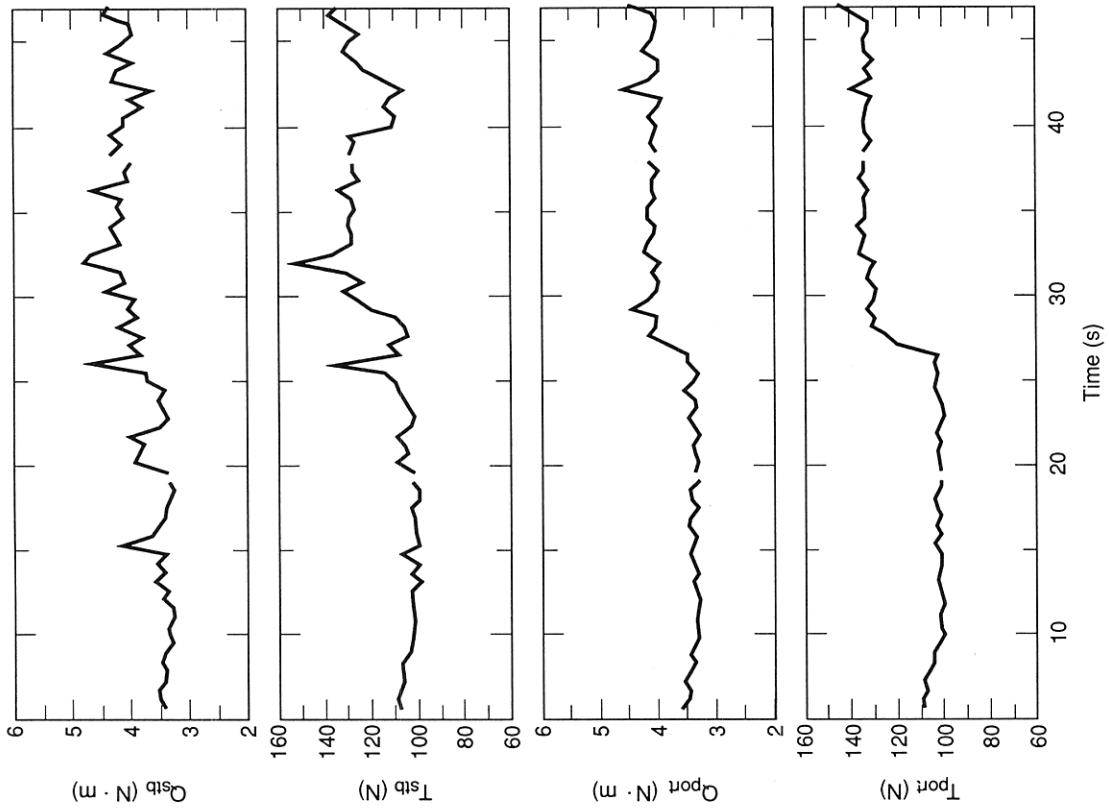


Figure 24. Time history of recorded signals during propulsion tests.



b. Test 502.
Figure 24 (cont'd).



c. Test 503.

Figure 24 (cont'd). Time history of recorded signals during propulsion tests.

Table 10. Results of propulsion tests in level ice ($h_i = 52 \text{ mm}$; $\sigma_f = 41 \text{ kPa}$; $V = 36 \text{ cm/s}$).

Test no.	n (rpm)	Pull (N)	Propeller thrust (N)		Propeller torque (N m)		P_d (W)
			Port	Starboard	Port	Starboard	
No ice interference							
501	490	-50.3	49.6	57.8	1.70	1.70	174.5
502	595	43.5	73.8	84.2	2.59	2.83	337.7
503	699	113.2	102.8	107.6	3.39	3.65	515.3
With ice interference							
501	490	-21.6	57.8	57.4	2.10	2.04	212.4
502	595	57.1	85.6	83.0	2.91	3.04	370.7
503	698	130.7	132.6	123.9	4.10	4.18	605.2

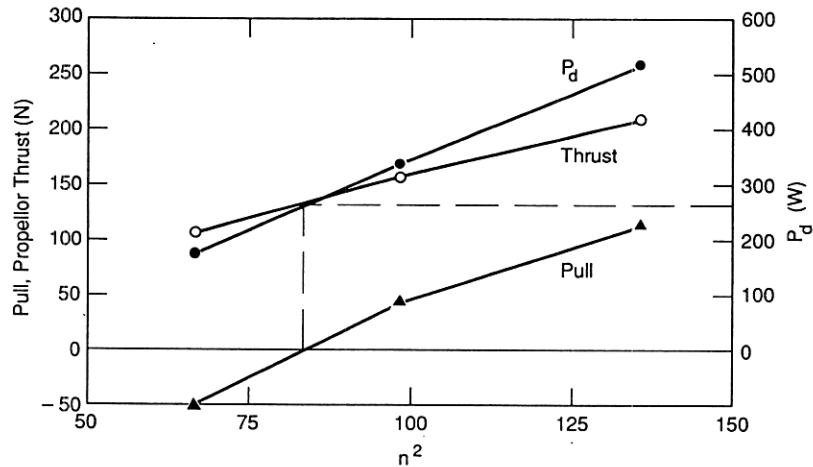


Figure 25. Results of model propulsion tests ($h_i = 52 \text{ mm}$; $\sigma_f = 41 \text{ kPa}$).

propeller speed at which the pull is zero. By interpolating the results obtained at 490 and 595 rpm, one can determine the self-propulsion point conditions at $V = 36 \text{ cm/s}$, $h_i = 50 \text{ m}$ to be

$$n_{sp} = 9.15 \text{ rps or } 550 \text{ rpm}$$

$$Q_{sp} = 2.25 \text{ N m (at each propeller)}$$

$$T_{sp} = 67.3 \text{ N (at each propeller)}$$

$$P_{sp} = 260 \text{ W.}$$

The no-interference condition was selected for determining the self-propulsion point because, as mentioned earlier, there is always significantly more ice-propeller interaction at model scale than at full scale owing to the smaller buoyancy of the model ice. Past experience (with the Canadian Coast Guard R-class icebreaker and the USCG bay class Great Lakes icebreaker) has also shown that full-scale predictions of power requirements in good agreement with field trial measurements are usually obtained when the model test data without ice interference are used.

However, it may be of interest to note that should the test data with ice interference be used to determine the model self-propulsion point, the corresponding propeller speed would decrease somewhat (to 8.8 rps) because of the thrust increase, but the delivered power would remain practically unchanged (258 W) because of the increase in torque.

FULL-SCALE PREDICTIONS

Direct extrapolation

The model ice sheet thickness and strength were extremely close to the target values. Therefore, one estimate of full-scale predictions at $V = 3 \text{ kn}$ (1.5 m/s) and $h_i = 3 \text{ ft}$ (0.9 m) can be obtained by straight extrapolation of the model self-propulsion conditions, that is

$$n_{FS} = 2.15 \text{ rps or } 129 \text{ rpm}$$

$$Q_{FS} = 246 \text{ kN m}$$

$$P_{FS} = 6.7 \text{ MW.}$$

Use of open-water propeller coefficients

The limited number of experiments carried out under the ice testing program, as well as other limitations, did not allow the determination of the nozzle thrust coefficient, of the overall deduction factor, or even of sufficiently accurate propeller coefficients. The open water characteristics of the propeller-duct combination used in the ice testing program were measured at the Institute for Marine Dynamics, St. John's, Newfoundland. They are listed in Appendix A and plotted on Figure A1.

The total thrust coefficient and the torque coefficient could be expressed as second degree polynomials of the advance coefficient, namely

$$K_{tt} = 0.507 - 0.677J - 0.0835J^2 \quad (r = 0.9999) \quad (16)$$

$$K_q = 0.0463 - 0.00852J - 0.0435J^2 \quad (r = 0.9999). \quad (17)$$

For the design conditions of $V = 3$ kn in 3 ft of level ice, the full-scale total ice resistance was predicted to be (Table 5)

$$R_{it} = 820 \text{ kN.}$$

If the thrust deduction factor is conservatively estimated at $t = 0.2$, then the thrust to be delivered by each propeller-nozzle combination is

$$T_t = \frac{R_{it}}{1-t} = 512.5 \text{ kN.}$$

Then, from eq 16, the required propeller speed is calculated to be $n = 2.24$ rps (134 rpm), and the corresponding advance coefficient is $J = 0.172$.

The torque on each propeller can be calculated from eq 17 to be

$$Q_p = 229.3 \text{ kN m}$$

and therefore the total delivered shaft power is

$$P_d = 6.44 \text{ MW.}$$

Use of SSPA test data

An extensive test program in ice-free water was carried out at SSPA, Gothenburg, Sweden. In this test program, the model propellers were stock CP propellers with a $P_{0.7}/D = 1.32$ instead of the 1.0 for the model propellers used in the ice tests. The open water coefficients, K_{tt} and K_q are shown vs J in Figure 26. In the range $0.1 < J < 0.25$, the thrust coefficient of one propeller-nozzle combination can be expressed as a linear function of J , namely

$$K_{tt} = 0.684 - 0.64J. \quad (18)$$

The propeller speed corresponding to $T_t = 512.5$ kN, as previously discussed, is calculated as

$$n = 1.90 \text{ s}^{-1} \text{ or } 114 \text{ rpm}$$

which yields an advance coefficient of

$$J = \frac{V}{nD} = 0.203.$$

From Figure 26, the corresponding value of $K_q = 0.07$, and the required shaft power is found to be

$$P_d = 6.4 \text{ MW.}$$

The three methods give estimates of required shaft power for the vessel to continuously break 3 ft of ice at 3 kn (0.9 m at 1.5 m/s) that are within 5% of each other and of the order of 6.5 MW, well below the 8.8 MW of shaft power that will be available.

BACKING TESTS

After the propulsion tests were completed, the ship

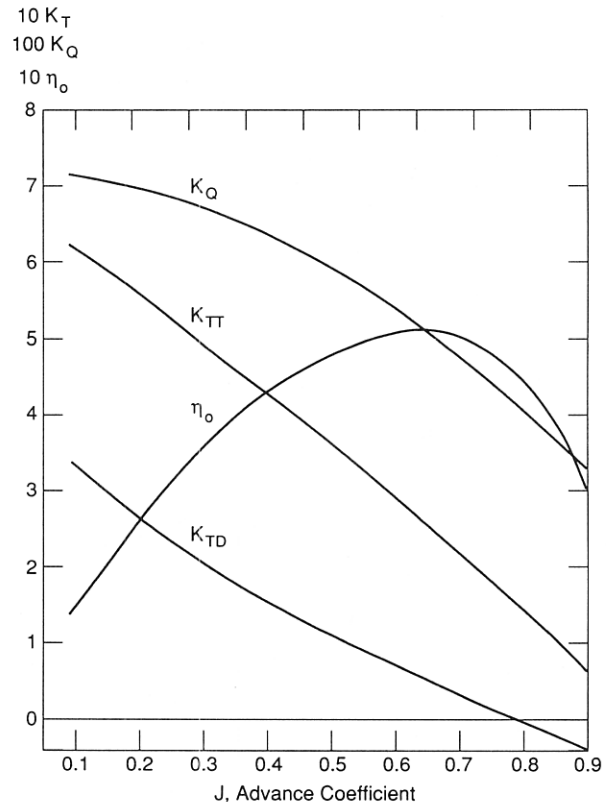


Figure 26. Propulsion characteristics (SSPA results).

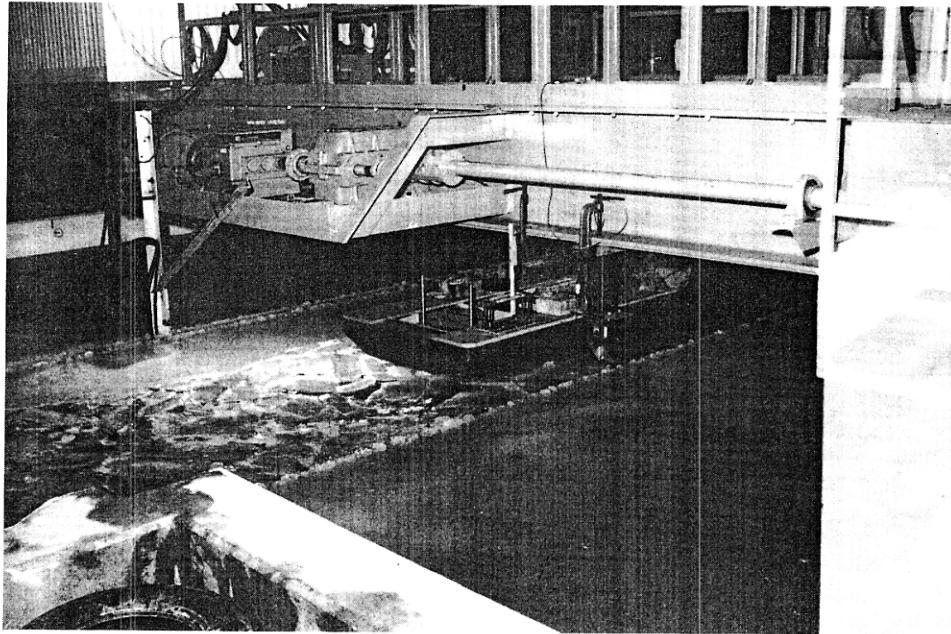
model was backed at a speed of 1.5 kn (0.8 m/s) full scale (18 cm/s at model scale) with the propellers running in reverse at about 115 rpm full scale (500 rpm at model scale). These tests were purely qualitative, for visual observations and video recordings. The model was first backed into brash ice, then into a section of level ice as shown in Figure 27. As expected, much ice was entrained through the nozzle and ground by the propellers, but the nozzles never became fully clogged.

RIDGE BREAKING TESTS

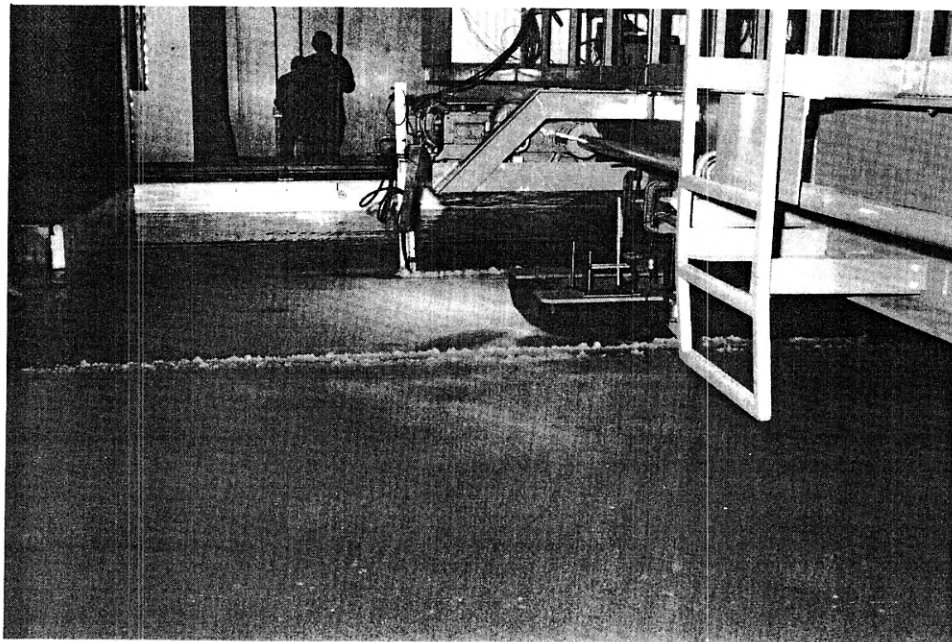
Ridge building procedures

The initial test program called for ramming tests in a ridge with a 6-ft (1.8-m) sail and a 20-ft (6.1-m) keel, full scale. No ridge length was specified. The charterer's representatives suggested a length of about one-third of the ship length.

After the propulsion tests were completed, a special-



a. In brash ice.



b. In level ice.

Figure 27. Backing tests.

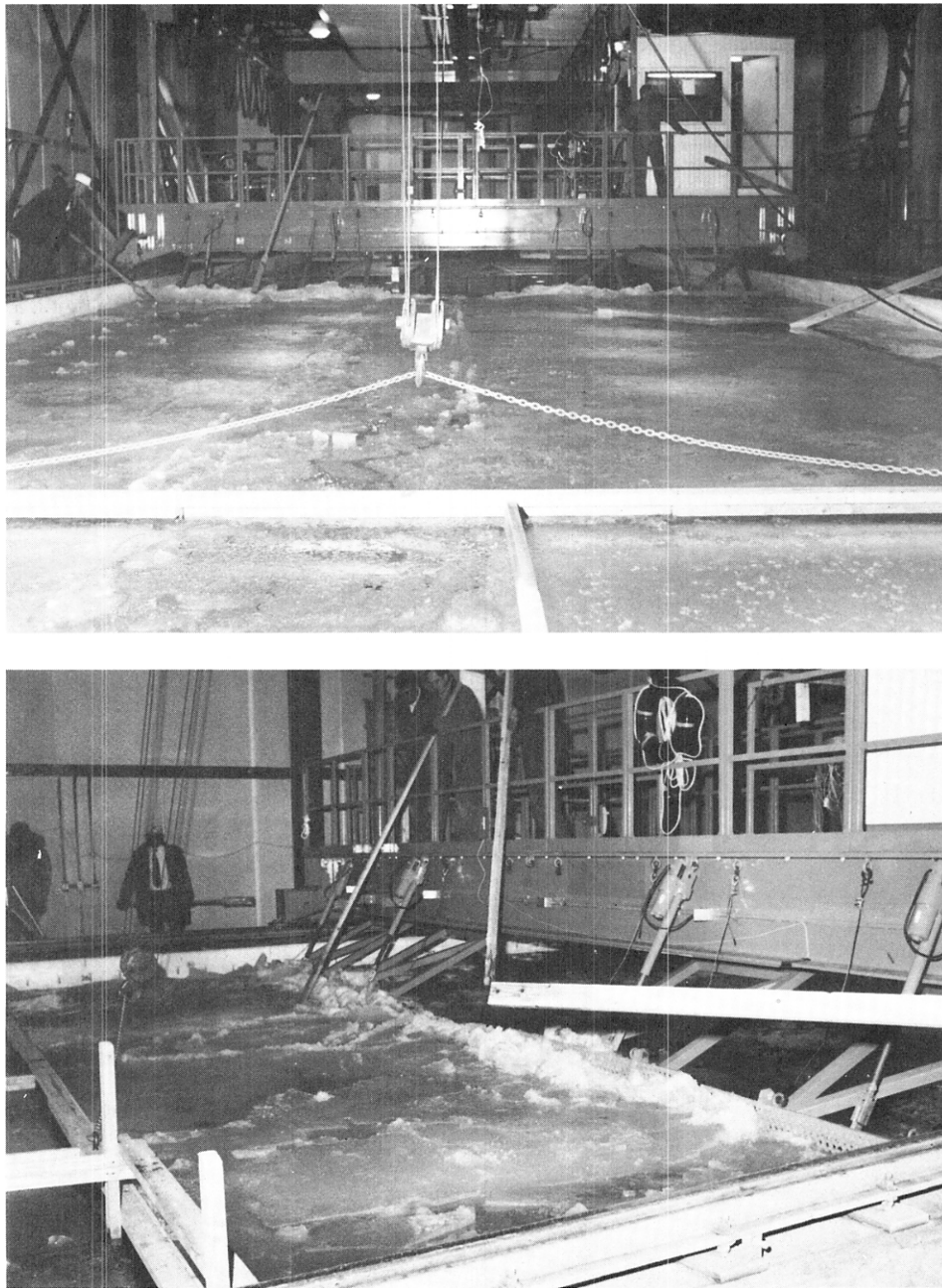


Figure 28. Ridge construction.

ly constructed retaining wall was mounted across the ice tank at about the 26-m mark, and secured to the side walls. The ice remaining in the tank between the 10- and 26-m marks was pushed against this retaining wall by the main carriage ice pushers (see Fig. 28). Two passes were necessary to complete the ridge, the length of which extended to about the 23.5-m mark. A second 2-ft-deep (0.60-m-deep) plywood wall was mounted across the tank to hold the ridge while the air temperature was

dropped to about 20°F (-7°C) to allow the ridge to become slightly reconsolidated for about 1½ hours.

The front wall was then removed. A slab of competent ice, 5 cm thick, the full width of the tank and 3 m long was then slowly pushed over the top of the ice rubble to simulate the reconsolidated ridge sail.

Finally, an additional 3-m-long, 5-cm-thick competent ice slab was pushed against the edge of the ridge to simulate an adjacent 3-ft (0.9-m) ice sheet. The back

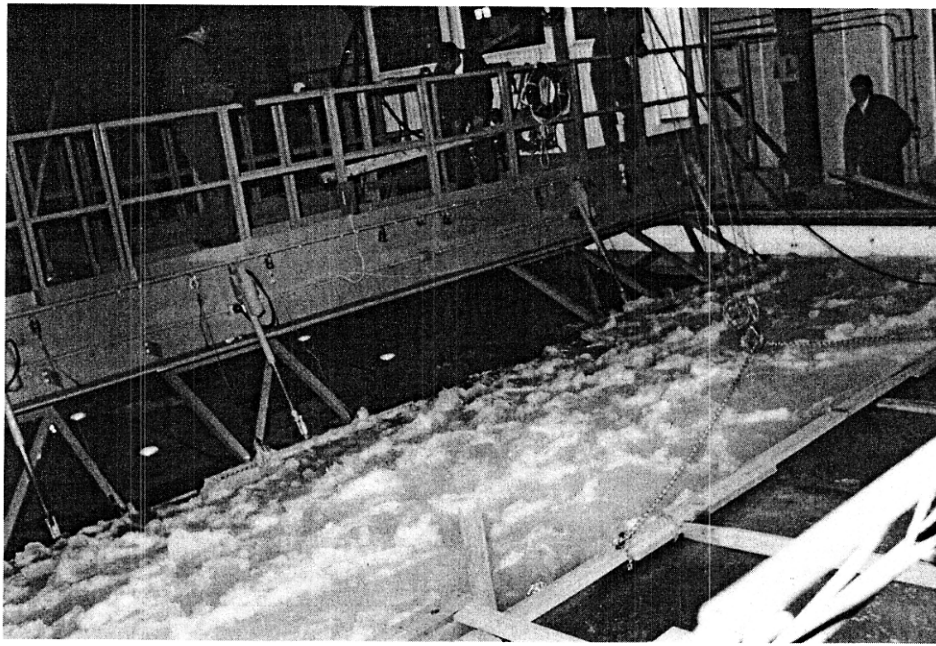


Figure 28 (cont'd).

retaining wall was removed, and the air temperature was allowed to rise to 34°F (1°C). Measuring rods were inserted every 0.5 m, and the ridge profile determined through the tank side windows as shown in Figure 29.

The final model ridge was 3 m long, or 64% of ship length, and had a 65-cm keel corresponding to a 38-ft (11.5-m) keel, full scale. Thus, the actual ridge dimensions far exceeded the test program requirements.

Test procedure

The ship model was fully disconnected from the towing tank except for the power cable and a tethering rope to prevent the model from exceeding the carriage velocity.

The ramming speed was to be 8 kn (4.1 m/s) full scale or 96 cm/s at model scale. The model propeller speed was set at 630 rpm, i.e., approximately at the intermediate point between full power at 8 kn in overload tests in open water and full power at bollard.

The carriage was then started at 72 cm/s. Initially, the ship model lagged behind the carriage, but, as it accelerated, it caught up with the carriage and was restrained by the tethering rope.

At the first ram, the ship model traveled through the 3 m of level ice ahead of the ridge, and through about three-quarters of the ridge before it stopped, as shown in Figures 30 and 31. At the second ram, the model broke through the full ridge (Fig. 32) and continued through the level ice beyond the ridge. Figure 33 shows an underwater view of the model nearly fully into the ridge.

RAMMING TESTS IN THICK, LEVEL ICE

The final tests required by the test program were ramming tests at 6 kn (3.1 m/s) full scale (72 cm/s, model scale) in 6-ft-thick (1.83-m-thick) ice (100 mm of model ice).

Once the model ice sheet had been grown and tempered, a 12-m-long, 1.20-m-wide channel was cut in the sheet to allow sufficient distance for model and carriage acceleration before impacting the ice.

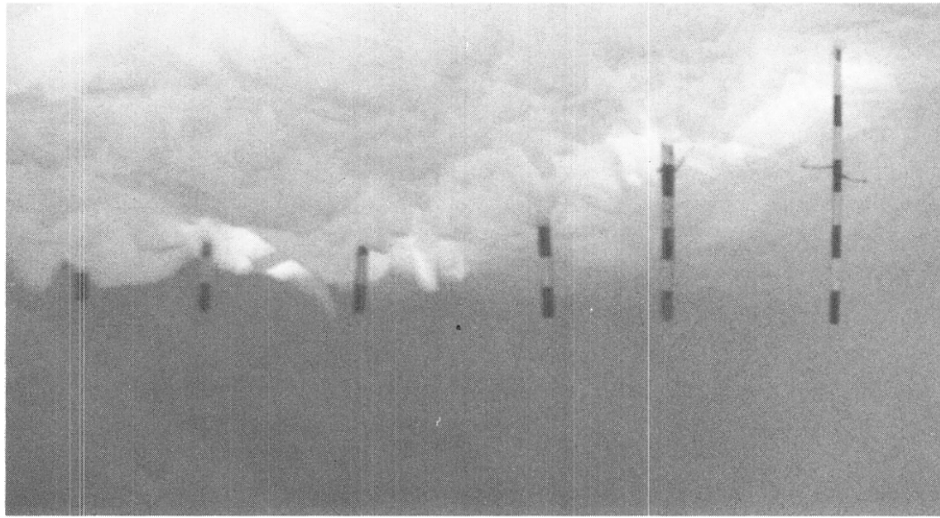
Even though the test program called only for one impact speed of 6 kn (3.1 m/s), impact velocities of 8 and 10 kn (4.1 and 5.1 m/s) were also tested.

The test procedure was similar to that of the ridge tests previously described, in that the ship model was connected to the carriage only by the power cable to the motor and by a tether.

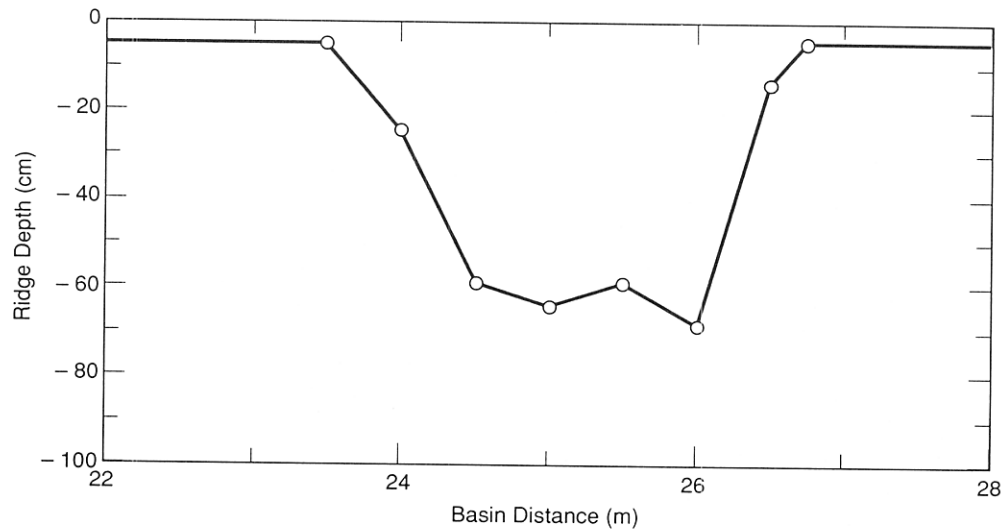
The propeller speed was usually set at the midway point between full power at bollard (600 rpm) and full power at the impact speed. However, for the tests at an impact velocity of 6 kn, the propeller speed was varied from 600 to 630 rpm.

After each ramming test, the penetration distance D_p of the model into the ice sheet was recorded. Photographs of a typical test and underwater views are shown in Figures 34 and 35. The test conditions and measured penetration distance are listed in Table 11 and depicted graphically in Figure 36.

From Figure 36, it can be seen that at the model impact speed of 72 cm/s, the penetration distance in-



a. Underwater view (all markers extend 90 cm below ridge top surface).



b. Measured profile.

Figure 29. Ridge profile.

creased linearly with increasing propeller speed. Similarly, the penetration distance was found to increase linearly with impact speed from an average of 40% of ship length at 6 kn full scale to nearly 80% of ship length at 10 kn (5.1 m/s).

Even these numbers may be conservative, since it was found in the course of the tests, and as previously mentioned in the section on ice properties measurements, that the ice was stronger than initially measured, namely 50 kPa as opposed to 42 kPa, but was only 90 mm thick, instead of the target of 100 mm. The change

Table 11. Results of ramming tests in thick level ice (D_p = penetration distance).

Test no.	V (cm/s)	n (rpm)	D_p (m)	D_p/LWL
601	72	615	2.50	0.54
602	72	630	2.20	0.47
603	72	600	1.55	0.33
604	72	615	1.77	0.38
605	120	630	3.70	0.79
606	96	625	2.85	0.61
607	72	615	1.85	0.40

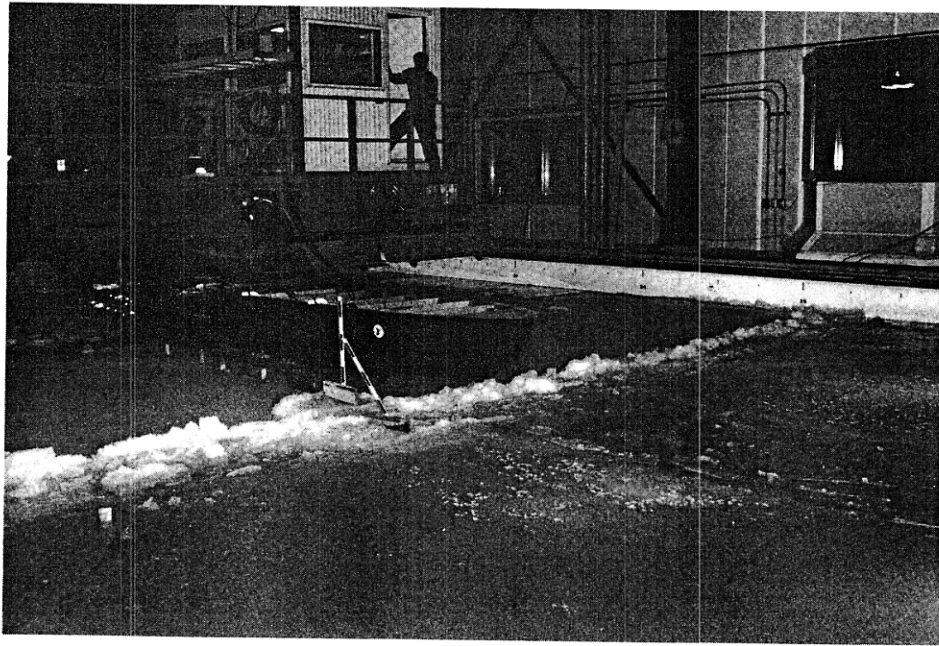


Figure 30. Model in ridge after first ram.

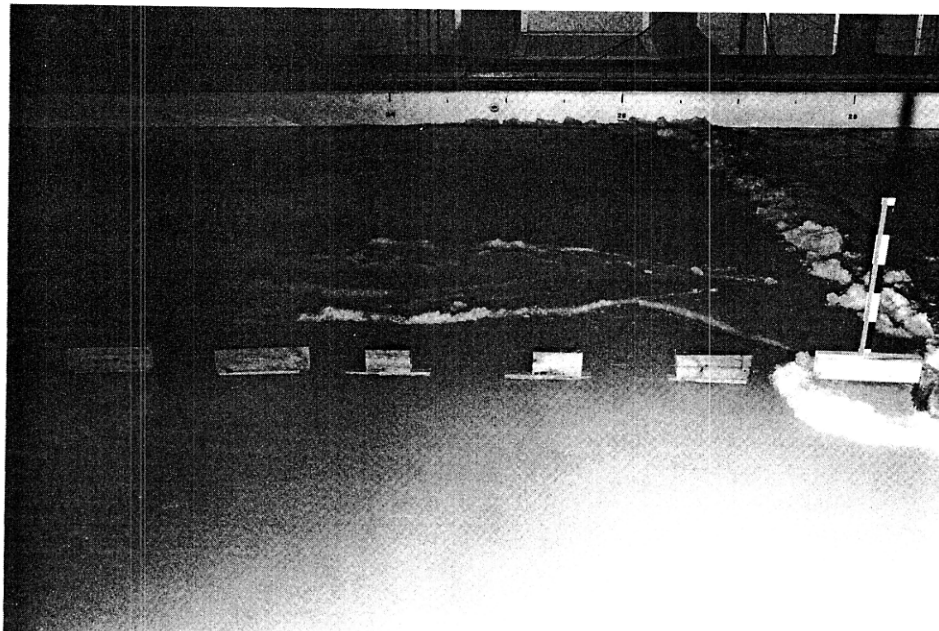


Figure 31. Imprint of model in ridge after first ram.

in ice strength, from 42 kPa near the trim tank to 50 kPa in the middle and back of the ice tank, may explain why the penetration distance measured in the first ramming test (no. 601) at $V = 72$ cm/s and 615 rpm was significantly greater than that measured in subsequent tests under identical conditions of impact speed and propeller rpm (test no. 604 and 607), namely 2.50 m as opposed to about 1.80 m.

CONCLUSIONS

From the results of the model test program in ice of the Antarctic research vessel, it can be concluded that:

1. The proposed 8.8 MW of power available at the propellers is more than sufficient to propel the ship continuously at 3 kn (1.5 m/s) through level, 3-ft-thick (0.9-m-thick) first year ice.

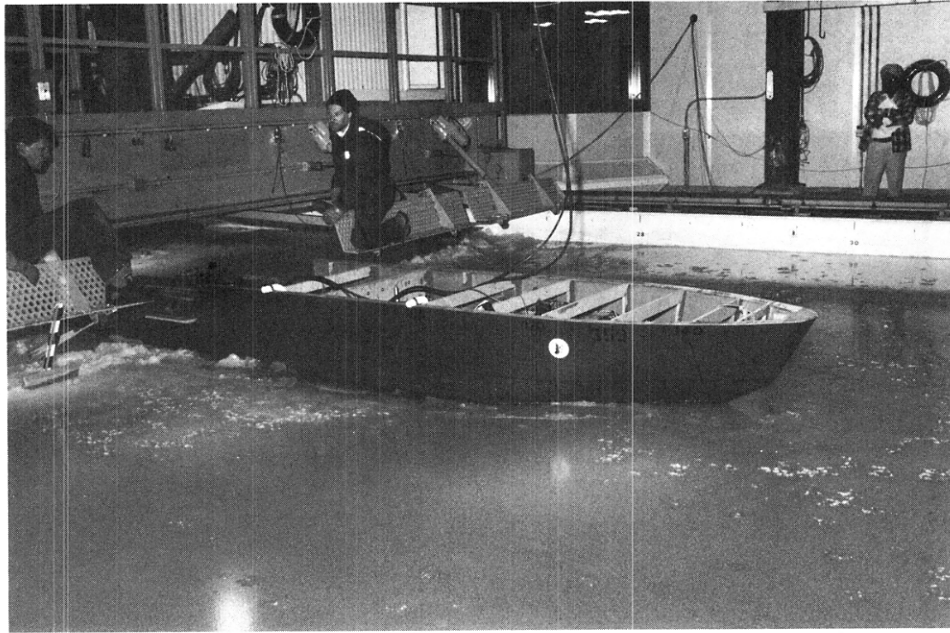


Figure 32. Model breaks through ridge at second ram.

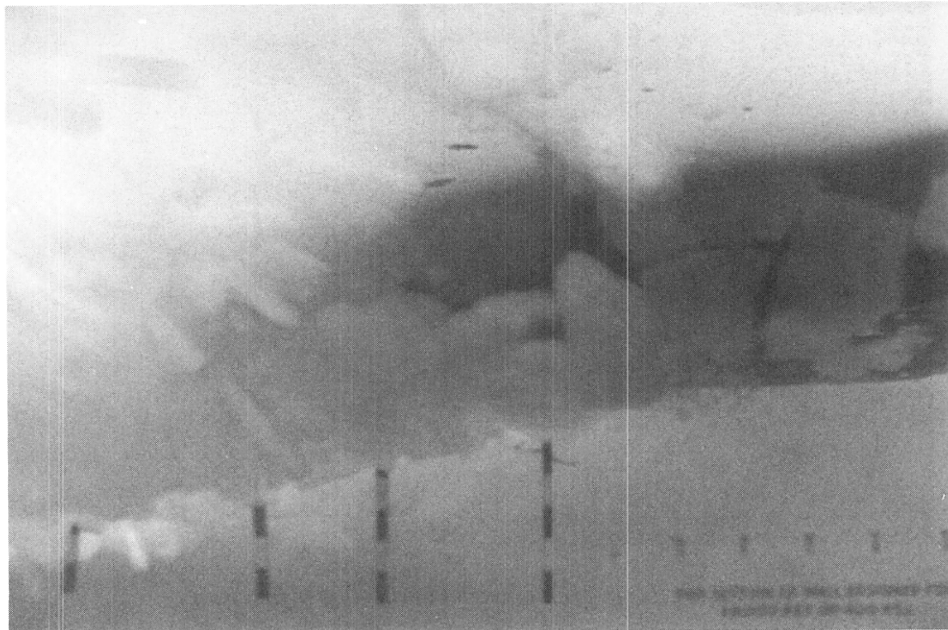
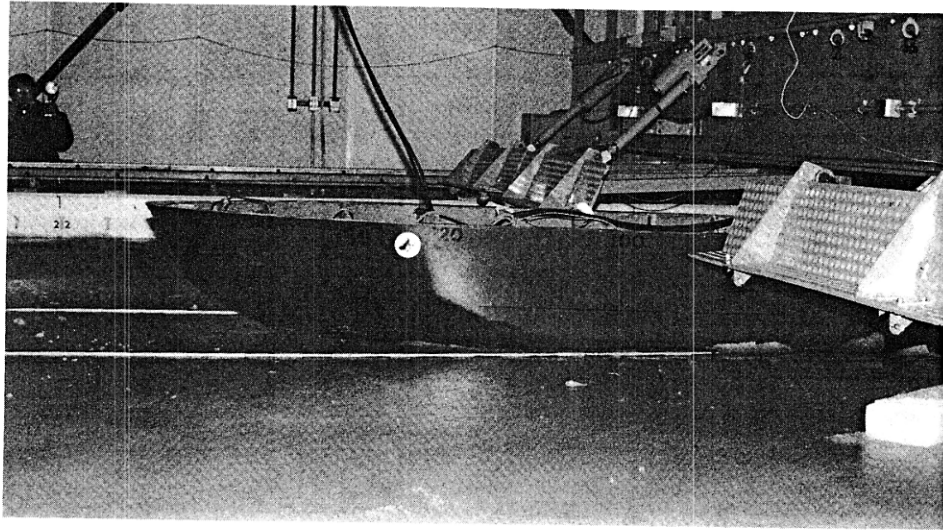


Figure 33. Underwater view of model in ridge.

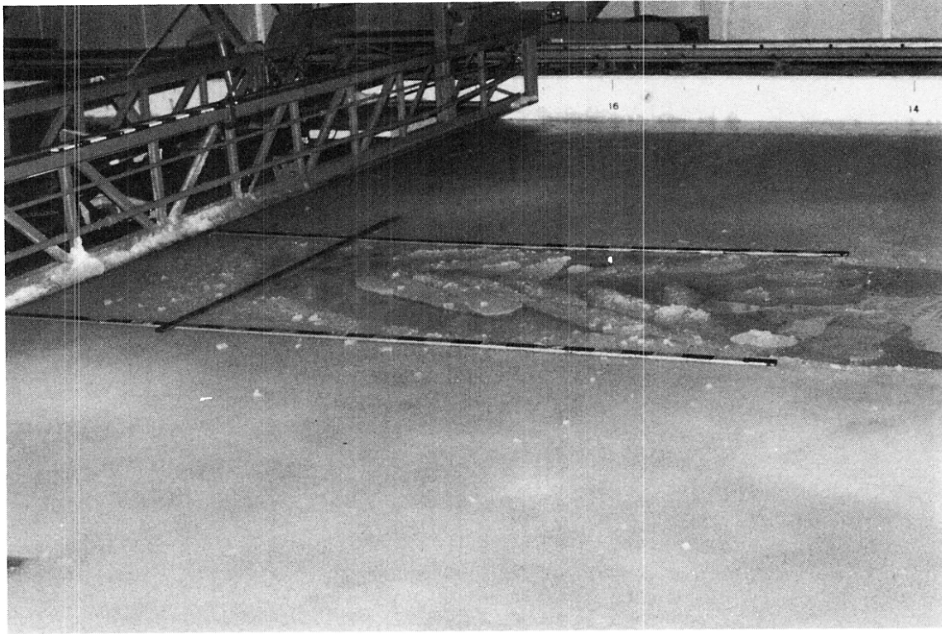


a. View of model.

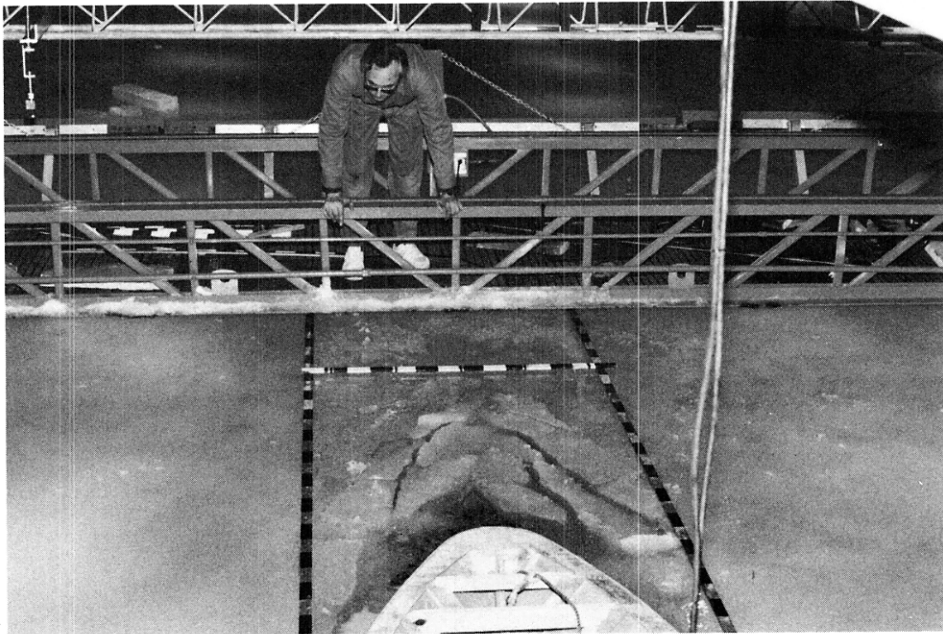


b. Top view of breaking pattern.

Figure 34. Ramming tests in 100-mm-thick ice (6-ft full-scale).



c. Side view of breaking pattern.



d. Measuring depth of penetration.

Figure 34 (cont'd). Ramming tests in 100-mm-thick ice (6-ft full-scale).

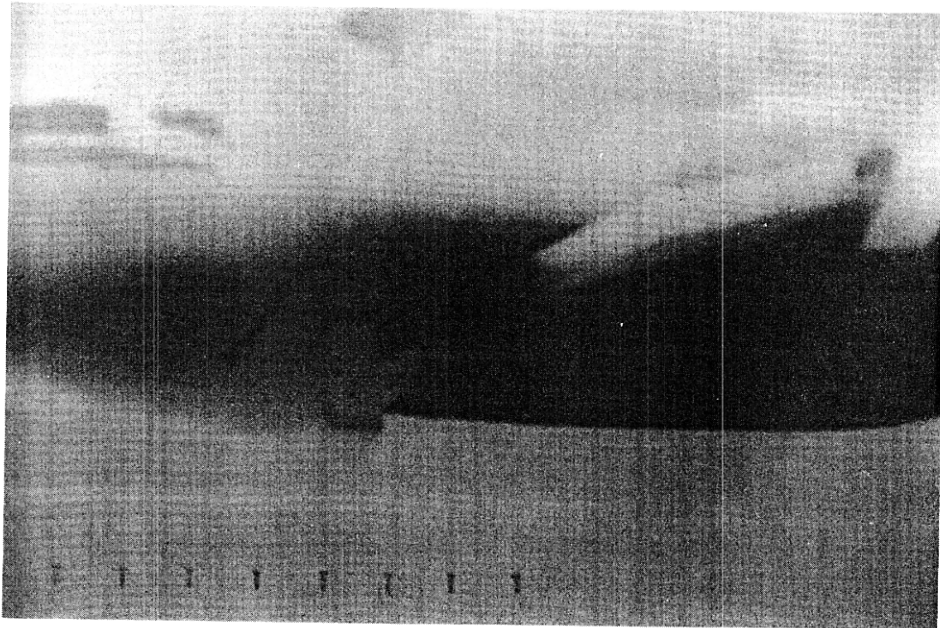
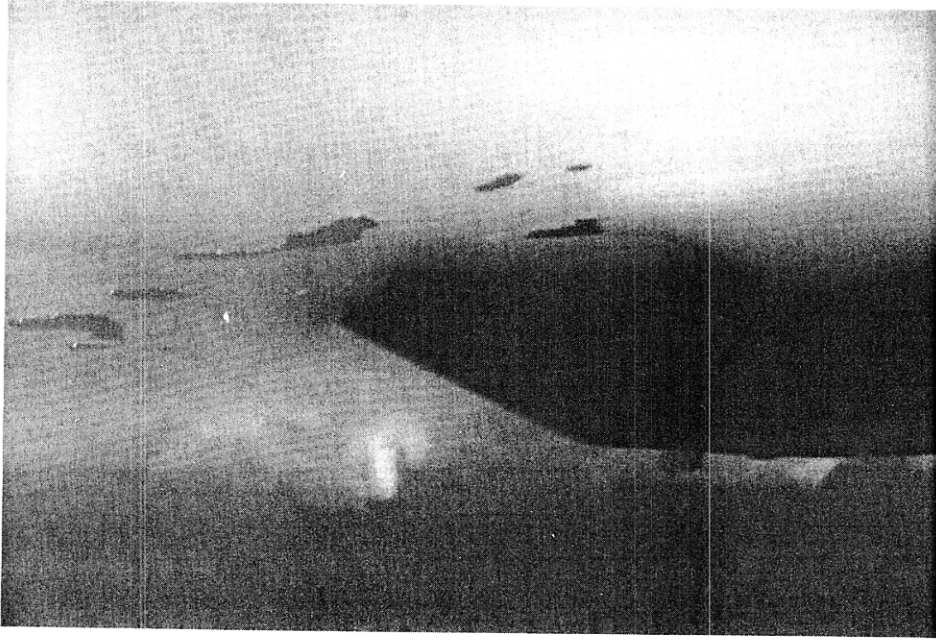


Figure 35. Underwater views during a ramming test.

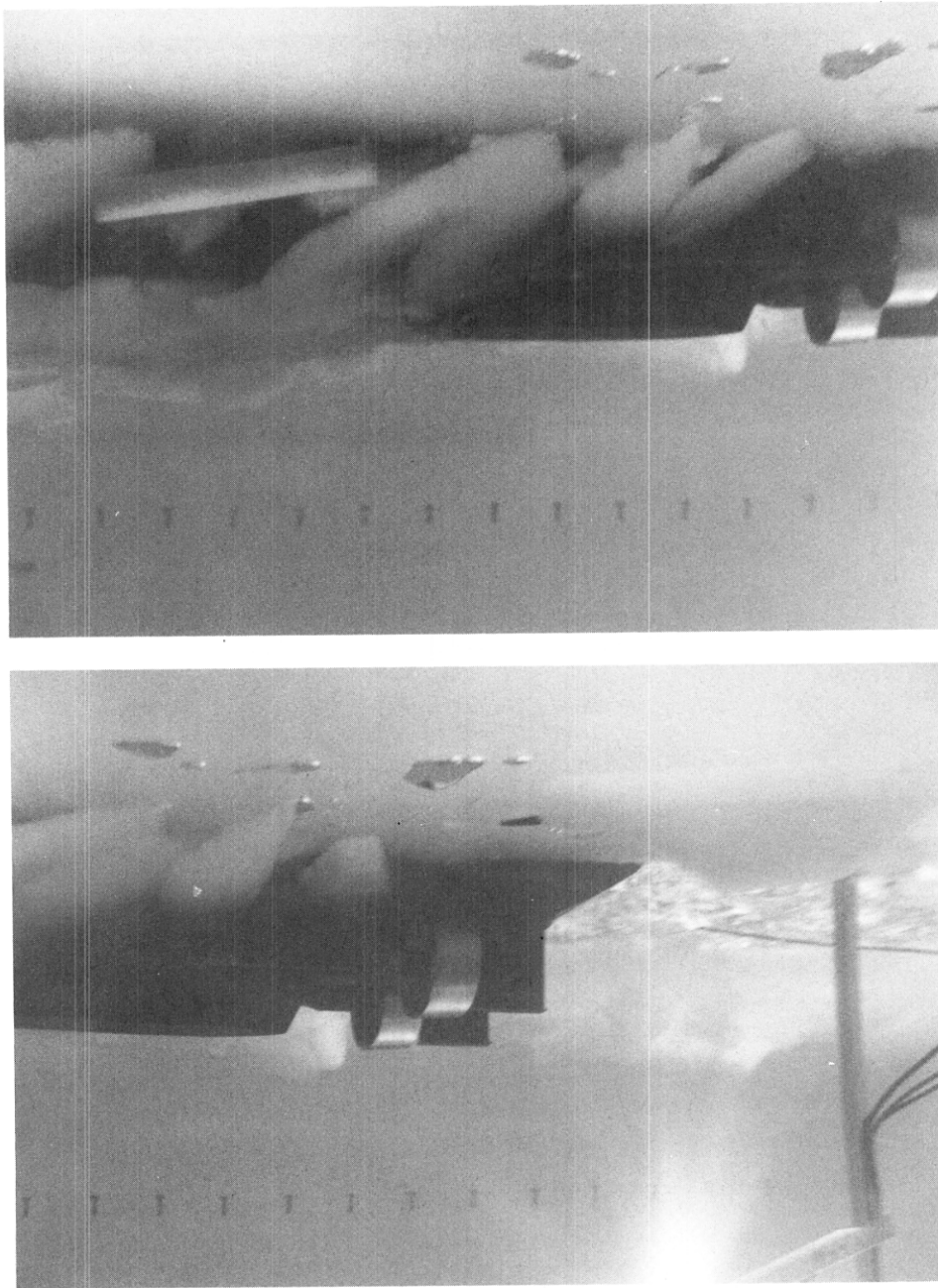


Figure 35 (cont'd). Underwater views during a ramming test.

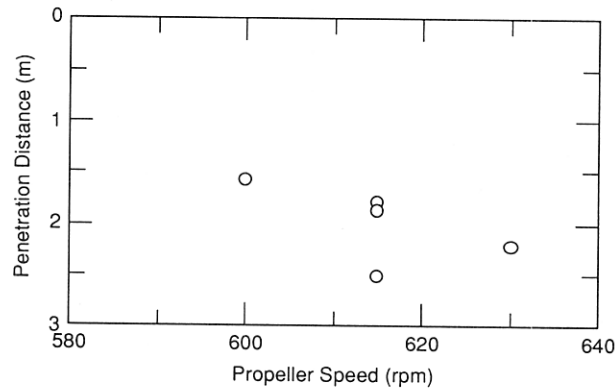
2. The vessel will be able to ram at a speed of 8 kn (4.1 m/s) through pressure ridges with 20-ft (6.1-m) or deeper keels.

3. When ramming in 6-ft-thick (1.8-m-thick) level ice, at an impact speed of 6 kn (3.1 m/s) at full power, the vessel is expected to penetrate by about one-third of a ship length into the ice.

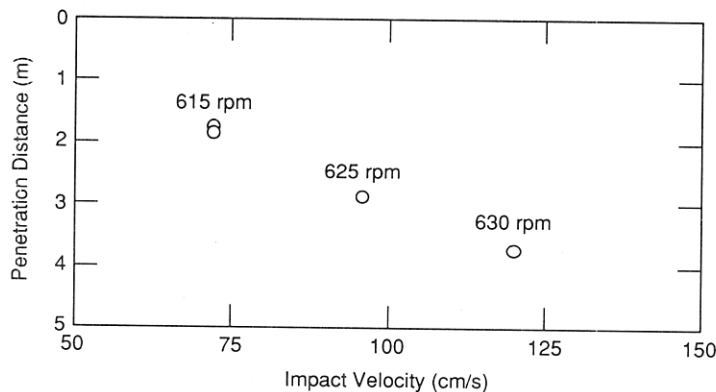
LITERATURE CITED

Colbourne, D.B. (1989) A three-component method for analyzing icebreaking resistance. Ph.D. Thesis, Memorial University of Newfoundland, St. John's, Newfoundland, Canada.

ITTC (1990) Report of the Performance in Ice-Covered



a. Effect of propeller speed on penetration depth ($V = 72$ cm/s or 6 kn full scale).



b. Effect of impact velocity on penetration depth.

Figure 36. Results of model ramming tests.

Waters Committee. In *Proceedings, 19th International Towing Tank Conference, Madrid, Spain, 16–22 September*, vol. I, p. 525–575.

Schwarz, J., Ed. (1979) IAHR: Recommendations on testing methods of ice properties. Research Report Tuleå 1979:03, Division of Water Resources, Engineering University of Luleå, Sweden.

Sodhi, D.S., C.R. Martinson, F.D. Haynes and K. Hirayama (1982) Determining the characteristic length of

model ice sheets. *Cold Regions Science and Technology*, 6: 99–104.

Tatinclaux, J.C. (1988) Ship model testing in level ice—An overview. USA Cold Regions Research and Engineering Laboratory, CRREL Report 88-15.

Tatinclaux, J.C. (1989) Effect of normal pressure on kinetic friction coefficient: Myth or reality? In *Proceedings, 22nd American Towing Tank Conference, St. John's, Newfoundland, 8–11 August*, p. 127–134.

**APPENDIX A: OPEN-WATER CHARACTERISTICS OF
PROPELLER-DUCT COMBINATION***

J	K_{tp}	K_{td}	K_{tt}	$10 K_q$	η_0
0.00	0.237	0.269	0.506	0.465	0.000
0.02	0.235	0.258	0.493	0.462	0.034
0.04	0.233	0.247	0.480	0.459	0.067
0.06	0.231	0.235	0.466	0.457	0.097
0.08	0.229	0.224	0.453	0.453	0.127
0.10	0.227	0.212	0.439	0.450	0.155
0.12	0.225	0.201	0.426	0.446	0.182
0.14	0.222	0.190	0.412	0.442	0.208
0.16	0.219	0.179	0.398	0.438	0.231
0.18	0.216	0.168	0.384	0.433	0.254
0.20	0.213	0.157	0.370	0.428	0.275
0.22	0.209	0.147	0.356	0.423	0.295
0.24	0.205	0.137	0.342	0.418	0.313
0.26	0.201	0.127	0.328	0.412	0.329
0.28	0.197	0.117	0.314	0.405	0.346
0.30	0.193	0.106	0.299	0.399	0.358
0.32	0.188	0.097	0.285	0.392	0.370
0.34	0.183	0.088	0.271	0.384	0.382
0.36	0.177	0.079	0.256	0.377	0.389
0.38	0.172	0.070	0.242	0.369	0.397
0.40	0.166	0.061	0.227	0.360	0.401
0.42	0.160	0.053	0.213	0.351	0.406
0.44	0.153	0.045	0.198	0.342	0.405
0.46	0.146	0.027	0.183	0.332	0.404
0.48	0.139	0.029	0.168	0.322	0.399
0.50	0.132	0.021	0.153	0.312	0.390
0.52	0.124	0.014	0.138	0.301	0.379
0.54	0.117	0.006	0.123	0.290	0.365
0.56	0.108	0.000	0.108	0.278	0.346
0.58	0.100	-0.007	0.093	0.267	0.322

* Institute for Marine Dynamics, St. John's, Newfoundland.

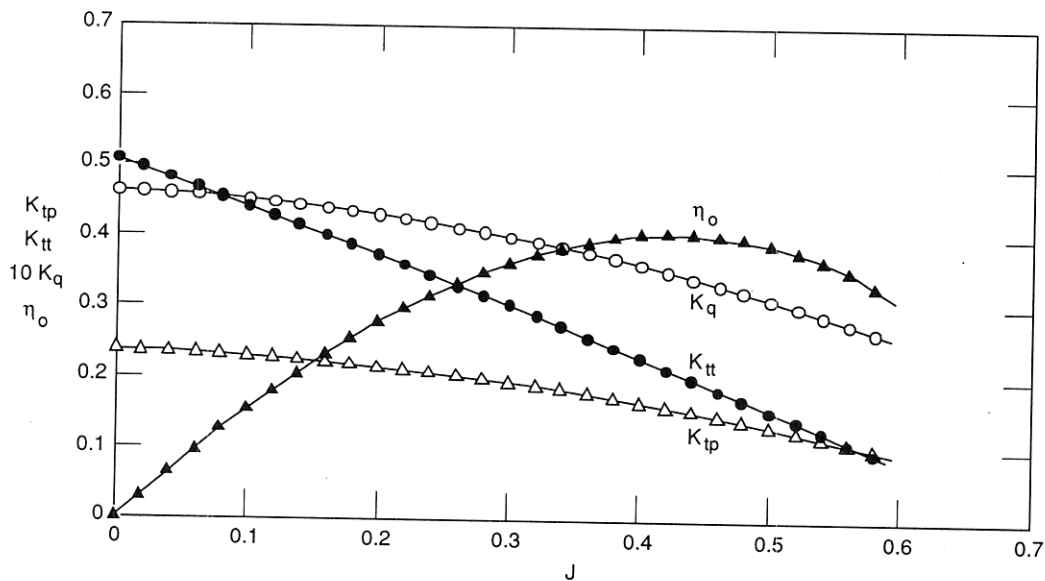


Figure A1. Open water propulsion coefficients for propeller-duct combination.

APPENDIX B: EFFECT OF TEST LENGTH ON MEASURED ICE RESISTANCE

When performing the resistance tests in level ice, it was assumed that one ship length in solid ice was a sufficient test length to obtain a valid measure of the total ice resistance, R_{it} . It was considered that the resistance R_{it} had reached its quasi-steady level after the ship model had penetrated into the solid ice by one-quarter to one-half of the waterline length LWL . Therefore, the force block output could be averaged over the remaining one-half to three-quarters of a ship length to obtain the mean ice resistance.

To verify the above assumption, one additional ice sheet was grown and a resistance test at the model speed of 36 cm/s (3 kn full scale) was made over 5 m (one ship length) of sawn ice followed by 13 m (3.5 ship lengths) of solid ice. The average ice thickness along the ship track was 53 ± 1.5 mm, and the ice flexural strength prior to the tests was 46 ± 5 kPa.

The time series of the carriage velocity and model resistance are shown in Figure B1. The resistance in sawn

ice was measured to be 36 N.

Averages of the resistance in solid ice were calculated over increasing distances ranging from 1.64 m or one third of the ship length to 10.8 m or 2.3 ship lengths. One set of averages was made after the model had penetrated 1.3 m (0.28 ship lengths) into the solid ice, another set after the model had penetrated by 2.3 m or half a ship length. In both cases, the averages varied between 147 and 155 N with no obvious increasing or decreasing trend with averaging distance.

These averages are shown graphically on Figure B2. The results of this additional resistance test show that, at least for the particular icebreaker hull under consideration, averages over one-half to three-quarters of a ship lengths after the model has penetrated by one-quarter to one-half of a length into solid ice yield representative and valid estimates of the mean ice resistance R_{it} and, therefore, that the test procedures were acceptable.

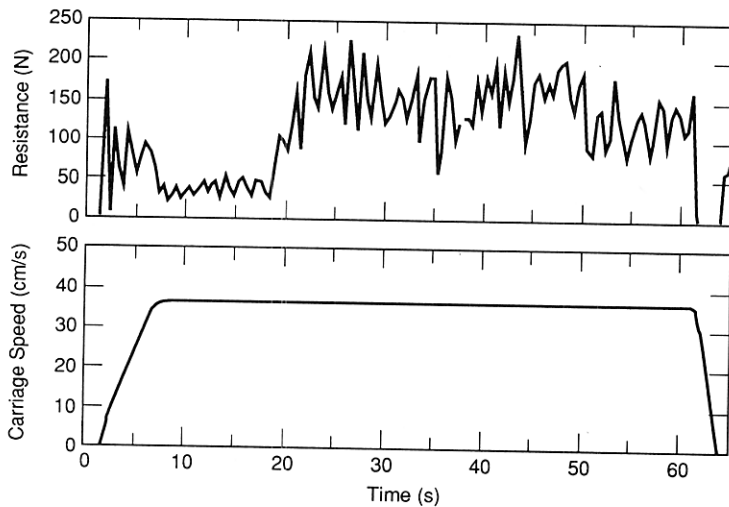


Figure B1. Time series of carriage speed and resistance for test 110.

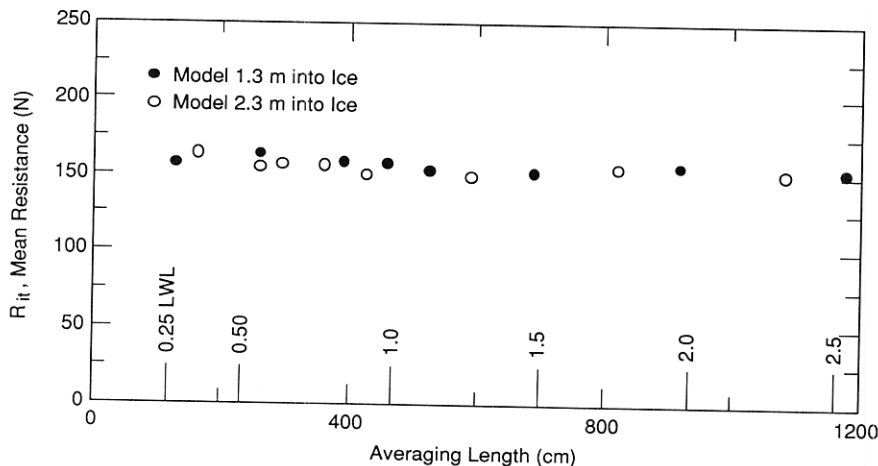


Figure B2. Effect of averaging length on mean resistance for test 110.

REPORT DOCUMENTATION PAGE

Form Approved
OMB No. 0704-0188

Public reporting burden for this collection of information is estimated to average 1 hour per response, including the time for reviewing instructions, searching existing data sources, gathering and maintaining the data needed, and completing and reviewing the collection of information. Send comments regarding this burden estimate or any other aspect of this collection of information, including suggestion for reducing this burden, to Washington Headquarters Services, Directorate for Information Operations and Reports, 1215 Jefferson Davis Highway, Suite 1204, Arlington, VA 22202-4302, and to the Office of Management and Budget, Paperwork Reduction Project (0704-0188), Washington, DC 20503.

1. AGENCY USE ONLY (Leave blank)		2. REPORT DATE February 1992		3. REPORT TYPE AND DATES COVERED	
4. TITLE AND SUBTITLE Tests in Ice on an Antarctic Research Vessel Model				5. FUNDING NUMBERS	
6. AUTHORS Jean-Claude Tatinclaux					
7. PERFORMING ORGANIZATION NAME(S) AND ADDRESS(ES) U.S. Army Cold Regions Research and Engineering Laboratory 72 Lyme Road Hanover, New Hampshire 03755-1290				8. PERFORMING ORGANIZATION REPORT NUMBER Special Report 92-3	
9. SPONSORING/MONITORING AGENCY NAME(S) AND ADDRESS(ES)				10. SPONSORING/MONITORING AGENCY REPORT NUMBER	
11. SUPPLEMENTARY NOTES					
12a. DISTRIBUTION/AVAILABILITY STATEMENT Approved for public release; distribution is unlimited. Available from NTIS, Springfield, Virginia 22161.				12b. DISTRIBUTION CODE	
13. ABSTRACT (<i>Maximum 200 words</i>) A new Antarctic research vessel to be chartered by the National Science Foundation was designed and is under construction by North American Shipbuilding, Inc., Larose, Louisiana. A full model test program was required by NSF to verify that the proposed design would meet the vessel operational requirements. In particular, the ship is to break 3 ft (0.9 m) of ice at 3 kn (1.5 m/s) continuously and break through pressure ridges with a 6-ft (1.8-m) sail and a 20-ft (6.1-m) keel. Ice model tests were made in CRREL's ice towing tank. The test program included resistance and propulsion tests in level ice, tests in ridges and ramming tests in ice floes of up to 6 ft (1.83 m) in thickness. The test results described in the report indicate that the proposed ship design with 8.8 MW of power available at the propeller would meet or exceed all operational requirements in ice: the power needed to operate continuously in 3-ft first year level ice at 3 kn was estimated at 6.5 MW; the vessel was found to be able to ram through a 38-ft (11-m) keel ridge; finally, when ramming in 6-ft thick level ice at an impact speed of 6 kn (3.1 m/s) at full power, the vessel was predicted to penetrate by about one-third of a ship length into the ice.					
14. SUBJECT TERMS Antarctica Icebreaker Ice ridge Level ice Model tests Ships				15. NUMBER OF PAGES 47	
				16. PRICE CODE	
17. SECURITY CLASSIFICATION OF REPORT UNCLASSIFIED		18. SECURITY CLASSIFICATION OF THIS PAGE UNCLASSIFIED		19. SECURITY CLASSIFICATION OF ABSTRACT UNCLASSIFIED	
				20. LIMITATION OF ABSTRACT UL	